



Search for a new Z' gauge boson in 4μ events with the ATLAS experiment

The ATLAS Collaboration

This paper presents a search for a new Z' vector gauge boson with the ATLAS experiment at the Large Hadron Collider using pp collision data collected at $\sqrt{s} = 13$ TeV, corresponding to an integrated luminosity of 139 fb^{-1} . The new gauge boson Z' is predicted by $L_\mu - L_\tau$ models to address observed phenomena that can not be explained by the Standard Model. The search examines the four-muon (4μ) final state, using a deep learning neural network classifier to separate the Z' signal from the Standard Model background events. The di-muon invariant masses in the 4μ events are used to extract the Z' resonance signature. No significant excess of events is observed over the predicted background. Upper limits at a 95% confidence level on the Z' production cross-section times the decay branching fraction of $pp \rightarrow Z' \mu\mu \rightarrow 4\mu$ are set from 0.31 to 4.3 fb for the Z' mass ranging from 5 to 81 GeV. The corresponding common coupling strengths, $g_{Z'}$, of the Z' boson to the second and third generation leptons above 0.003 – 0.2 have been excluded.

1 Introduction

This paper presents a search for a new vector boson Z' in the four-muon (4μ) final state with data recorded in proton-proton (pp) collisions at $\sqrt{s} = 13$ TeV by the ATLAS detector [1] at the Large Hadron Collider (LHC), corresponding to an integrated luminosity of 139 fb^{-1} . The new gauge boson Z' , which only interacts with the second and third generation leptons, is predicted by $L_\mu - L_\tau$ models [2] which extend the Standard Model (SM) with an additional $U(1)_{L_\mu - L_\tau}$ symmetry to address the observed anomalies of the muon magnetic dipole moment ($g - 2$) [3–6] and of rare B decays [7–10]. These models also aim to probe outstanding physics questions related to dark matter and neutrino mass [11–13].

The Z' kinematics, mass, and interactions (with the same coupling strength to the second and third lepton families), are described by the Lagrangian below:

$$L_{Z'} = -\frac{1}{4}F_{\alpha\beta}F^{\alpha\beta} + \frac{1}{2}M_{Z'}^2 Z'_\alpha Z'^\alpha - g_{Z'} Z'_\alpha (\bar{\ell}_2 \gamma^\alpha \ell_2 + \bar{\mu} \gamma^\alpha \mu - \bar{\ell}_3 \gamma^\alpha \ell_3 - \bar{\tau} \gamma^\alpha \tau),$$

where $F_{\alpha\beta} = \partial_\alpha Z'_\beta - \partial_\beta Z'_\alpha$ is the Z' field strength tensor; $\ell_i = (\nu_i, e_i)^T$ ($i = 2, 3$, denoting the second and the third generation left-handed lepton doublets); μ and τ represent the right-handed muon and tau singlets; and $g_{Z'}$ (which will be referred to as g in the rest of this paper) is the interaction coupling constant. The parameter space of $(m_{Z'}, g)$ has not been strongly constrained in experiments since the Z' does not directly couple to the electron nor to any quarks, hence it could not be directly produced from e^+e^- and pp colliding beams.

In pp collisions at the LHC, the Z' could be produced from final state radiation of μ or τ pairs of the Drell-Yan (DY) process as shown in Figure 1(a) with a 4μ final state, which provides the cleanest signature to search for the Z' . For relatively low Z' mass, the most promising experimental signature would be an excess of 4μ events with the invariant mass of one $\mu^+\mu^-$ pair peaking around the Z' mass. The major background comes from the SM 4μ production processes shown in Figure 1(b) to 1(d). The Z' could also be produced in W production through the DY process, $pp \rightarrow W \rightarrow Z'\mu\nu \rightarrow 3\mu + \nu$. The experimental signature would have a final state of 3μ plus large missing transverse energy. This final state is not included in this analysis.

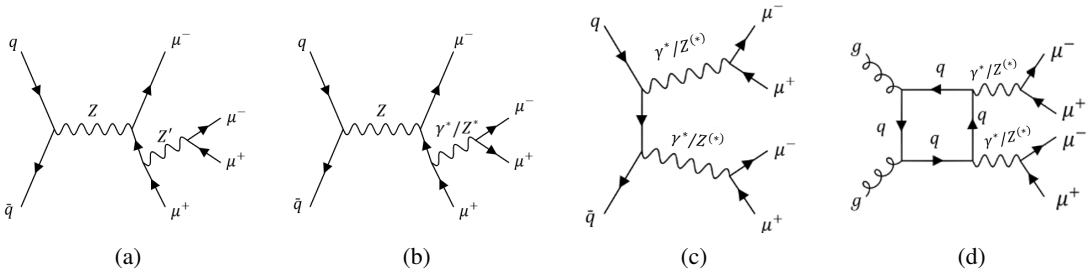


Figure 1: Feynman diagrams of Z' production through radiation in a Drell-Yan process (a), and of the corresponding SM background processes (b - d) with a 4μ final state.

Both the ATLAS and CMS Collaborations have measured the cross-sections of the SM $Z \rightarrow 4\mu$ process [14–16]. The measurement by ATLAS was used by theorists to set limits in the parameter

space of the $L_\mu - L_\tau$ model [11]. The CMS Collaboration has directly searched for the Z' boson in the mass region between 5 to 70 GeV with the 4μ final state using 77.3 fb^{-1} of data [17], and set upper limits on the Z' to muon coupling strength, g , of $0.004 - 0.3$ at 95% confidence level, depending on the Z' mass.

The organization of this paper is as follows. The ATLAS detector is described in the next section. The dataset and Monte Carlo samples used in this analysis are detailed in Section 3. Event reconstruction and selection, followed by background estimation from data, are described in Section 4 and Section 5. Event classification using a deep learning approach is presented in Section 6. Systematic uncertainties and the statistical approach to interpret data to obtain the results are reported in Section 7 and Section 8. The conclusion is given in the final section.

2 ATLAS Detector

The ATLAS detector [1] at the LHC covers nearly the entire solid angle around the collision point.¹ It consists of an inner tracking detector surrounded by a thin superconducting solenoid, electromagnetic and hadron calorimeters, and a muon spectrometer incorporating three large superconducting air-core toroidal magnets.

The inner-detector system (ID) is immersed in a 2 T axial magnetic field and provides charged-particle tracking in the range $|\eta| < 2.5$. The high-granularity silicon pixel detector covers the vertex region and typically provides four measurements per track, the first hit normally being in the insertable B-layer (IBL) installed before Run 2 [18, 19]. It is followed by the silicon microstrip tracker (SCT), which usually provides eight measurements per track. These silicon detectors are complemented by the transition radiation tracker (TRT), which enables radially extended track reconstruction up to $|\eta| = 2.0$. The TRT also provides electron identification information based on the fraction of hits (typically 30 in total) above a higher energy-deposit threshold corresponding to transition radiation.

The calorimeter system covers the pseudorapidity range $|\eta| < 4.9$. Within the region $|\eta| < 3.2$, electromagnetic calorimetry is provided by barrel and endcap high-granularity lead/liquid-argon (LAr) calorimeters, with an additional thin LAr presampler covering $|\eta| < 1.8$ to correct for energy loss in material upstream of the calorimeters. Hadron calorimetry is provided by the steel/scintillator-tile calorimeter, segmented into three barrel structures within $|\eta| < 1.7$, and two copper/LAr hadron endcap calorimeters. The solid angle coverage is completed with forward copper/LAr and tungsten/LAr calorimeter modules optimised for electromagnetic and hadronic energy measurements respectively.

¹ ATLAS uses a right-handed coordinate system with its origin at the nominal interaction point (IP) in the centre of the detector and the z -axis along the beam pipe. The x -axis points from the IP to the centre of the LHC ring, and the y -axis points upwards. Cylindrical coordinates (r, ϕ) are used in the transverse plane, ϕ being the azimuthal angle around the z -axis. The pseudorapidity is defined in terms of the polar angle θ as $\eta = -\ln \tan(\theta/2)$. Angular distance is measured in units of $\Delta R \equiv \sqrt{(\Delta\eta)^2 + (\Delta\phi)^2}$.

The muon spectrometer (MS) comprises separate trigger and high-precision tracking chambers measuring the deflection of muons in a magnetic field generated by the superconducting air-core toroidal magnets. The field integral of the toroids ranges between 2.0 and 6.0 T m across most of the detector. Three layers of precision chambers, each consisting of layers of monitored drift tubes, covers the region $|\eta| < 2.7$, complemented by cathode-strip chambers in the forward region, where the background is highest. The muon trigger system covers the range $|\eta| < 2.4$ with resistive-plate chambers in the barrel, and thin-gap chambers in the endcap regions.

Interesting events are selected by the first-level trigger system implemented in custom hardware, followed by selections made by algorithms implemented in software in the high-level trigger [20]. The first-level trigger accepts events from the 40 MHz bunch crossings at a rate below 100 kHz, which the high-level trigger further reduces in order to record events to disk at about 1 kHz.

An extensive software suite [21] is used in data simulation, in the reconstruction and analysis of real and simulated data, in detector operations, and in the trigger and data acquisition systems of the experiment.

3 Dataset and Monte Carlo Simulations

The data used for this analysis were recorded using single-muon and multi-muon triggers, corresponding to an integrated luminosity of 139 fb^{-1} after the application of data quality requirements [22]. The transverse momentum (p_T) thresholds for the single-muon trigger vary from 20 to 26 GeV, for the di-muon trigger from 10 to 14 GeV, and for the tri-muon trigger from 4 to 6 GeV, depending on the data-taking periods [23]. The overall trigger efficiency in the phase space defined by the event selections used in this analysis is higher than 98%.

3.1 Simulation of Z' Production

The $L_\mu - L_\tau$ model is used for Monte Carlo (MC) Z' signal sample production, where the Z' couples to the left-handed (LH) muon or tau leptons and their corresponding neutrinos, and to the right-handed (RH) muon or tau leptons. In the model, the Z' couplings to the first lepton families (electron and its neutrino) and all quarks are set to zero. The branching fractions of the Z' decay to a pair of muons and a pair of muon neutrinos are $\frac{1}{3}$ and $\frac{1}{6}$, respectively. The signal from tau decays in the 4μ final state is found to be negligible in this analysis and is not included as signal.

The interactions [24] mediated by a resonance Z' which couples to the second and third generation leptons are used for four-muon signal event generation. The signal events are generated with MADGRAPH5_aMC@NLO 2.7.3 [25] at leading-order (LO) accuracy in QCD by using the *Universal FeynRules Output* (UFO) format [26, 27]. Based on theoretical calculations [28, 29] for related processes, the appropriate NNLO/LO correction factor K of 1.3 is used to correct the MC LO signal cross-sections. In the signal production simulations, the NNPDF2.3_{NLO} set [30] is used for parton distribution function (PDF) for the pp collisions. PHOTOS++ 3.61 [31, 32] is used to simulate the effect of QED final-state radiation.

The MC simulated events are generated for a range of masses and coupling parameters of the $L_\mu - L_\tau$ model. The Z' mass ranges from 5 to 81 GeV, and the value of coupling constant g ranges from 0.008 to 0.316, as summarized in Table 1. The value of the g at each Z' mass was chosen to be close to the expected experimental sensitivity to allow a sensitive search for a very small Z' signal in the full Run 2 dataset.

With the chosen g , the natural width Γ of the Z' and the cross-section, both are proportional to g^2 , are calculated as listed in Table 1. It should be noted that all the generated mass points have the ratio $\Gamma/m_{Z'}$ much smaller than 1%. Therefore, the ATLAS detector mass resolution (2%) dominates the width of the signal Z' mass peak in the experimental dimuon mass spectrum.

Table 1: Summary of the chosen Z' hypotheses and corresponding coupling, width, and cross-section $\sigma(pp \rightarrow Z'\mu^+\mu^- \rightarrow \mu^+\mu^-\mu^+\mu^-)$, calculated at LO accuracy in QCD, at each mass point.

$m_{Z'}$ [GeV]	g	Γ [GeV]	σ [fb]	$m_{Z'}$ [GeV]	g	Γ [GeV]	σ [fb]
5	0.0080	2.45×10^{-5}	9.96	42	0.0900	2.71×10^{-2}	13.38
7	0.0085	3.99×10^{-5}	7.06	45	0.1000	3.58×10^{-2}	11.72
9	0.0090	5.78×10^{-5}	5.60	48	0.1100	4.62×10^{-2}	9.96
11	0.0095	7.89×10^{-5}	4.65	51	0.1200	5.84×10^{-2}	8.24
13	0.0100	1.03×10^{-4}	3.95	54	0.1600	1.10×10^{-1}	10.07
15	0.0120	1.72×10^{-4}	4.45	57	0.2000	1.81×10^{-1}	10.73
17	0.0140	2.65×10^{-4}	4.80	60	0.2665	3.39×10^{-1}	12.92
19	0.0160	3.87×10^{-4}	5.00	63	0.2680	3.60×10^{-1}	8.84
23	0.0240	1.05×10^{-3}	7.30	66	0.2780	4.06×10^{-1}	6.50
27	0.0320	2.20×10^{-3}	8.50	69	0.2890	4.59×10^{-1}	4.89
31	0.0400	3.95×10^{-3}	8.72	72	0.3000	5.15×10^{-1}	3.80
35	0.0600	1.00×10^{-2}	12.82	75	0.3000	5.37×10^{-1}	2.88
39	0.0800	1.99×10^{-2}	14.77	78	0.3080	5.89×10^{-1}	2.40
				81	0.3160	6.44×10^{-1}	2.08

The Z' signal samples were simulated with the ATLAS fast simulation framework (Atlfast-II) [33] to produce predictions that can be directly compared with the data.

3.2 Simulation of Background Events

Dominant SM backgrounds in this analysis come from the SM $Z \rightarrow 4\mu$ processes where the four leptons have an invariant mass close to that of the Z boson. In the higher mass region the ZZ^* production contributes a sizable number of prompt 4μ events. In addition, there are very small contributions from the Higgs boson, $t\bar{t}V$ ($V = W, Z$), and tri-boson (VVV) production processes. These events are estimated with MC simulations. The background events including muons from heavy-flavour hadron decays, misidentified jets, or photon conversions (collectively referred to as “non-prompt muon background”) are mostly coming from $Z + \text{jets}$, $t\bar{t}$ and single-top-quark production processes and estimated from data in this analysis, as described in Section 5. The $Z + \text{jets}$ and $t\bar{t}$ MC samples are also produced for background studies.

Samples of diboson production $q\bar{q} \rightarrow VV^{(*)}$, including the processes shown in Figures 1(b) and 1(c), were simulated with the SHERPA 2.2.2 [34] generator, including off-shell effects and Higgs boson contributions, where appropriate. Fully leptonic final states and semileptonic final states, where one boson decays leptonically and the other hadronically, were generated using matrix elements at next-to-leading-order (NLO) accuracy in QCD for up to one additional parton and at LO accuracy for up to three additional parton emissions. Samples for the loop-induced processes $gg \rightarrow ZZ^{(*)}$, shown in Figure 1(d), were generated using LO-accurate matrix elements for up to one additional parton emission for both the cases of fully leptonic and semileptonic final states. The matrix element calculations were matched and merged with the SHERPA parton shower based on Catani–Seymour dipole factorisation [35, 36] using the MEPS@NLO prescription [37–40]. The virtual QCD corrections were provided by the OPENLOOPS library [41–43]. The NNPDF3.0_{NNLO} set of PDFs was used [44], along with the dedicated set of parton-shower parameters (tune) developed by the SHERPA authors.

The production of $t\bar{t}$ events was modelled using the POWHEG BOX v2 [45–48] generator at NLO in QCD with the NNPDF3.0_{NLO} PDF set and the h_{damp} parameter² set to $1.5 m_{\text{top}}$ [49]. The events were interfaced to PYTHIA 8.230 [50] to model the parton shower, hadronisation, and underlying event, with parameters set according to the A14 tune [51] and using the NNPDF2.3_{LO} set of PDFs. The associated production of top quarks with W bosons (tW) was modelled by the POWHEG BOX v2 [46–48, 52] generator at NLO in QCD using the five-flavour scheme and the NNPDF3.0_{NLO} set of PDFs. The diagram removal scheme [53] was used to remove interference and overlap with $t\bar{t}$ production. The events were interfaced to PYTHIA 8.230 using the A14 tune and the NNPDF2.3_{LO} set of PDFs.

The production of V -jets was simulated with the SHERPA 2.2.1 generator using NLO matrix elements for up to two partons, and LO matrix elements for up to four partons, calculated with the Comix and OPENLOOPS libraries. They were matched with the SHERPA parton shower using the MEPS@NLO prescription with the set of tuned parameters developed by the SHERPA authors. The NNPDF3.0_{NNLO} set of PDFs was used and the samples were normalised to a next-to-next-to-leading-order (NNLO) prediction [54].

The production of $t\bar{t}V$ events was modelled using the MADGRAPH5_aMC@NLO 2.3.3 generator at NLO with the NNPDF3.0_{NLO} PDF. The events were interfaced to PYTHIA 8.210 using the A14 tune and the NNPDF2.3_{LO} PDF set. The production of tri-boson (VVV) events was simulated with the SHERPA 2.2.2 generator. Matrix elements accurate to LO in QCD for up to one additional parton emission were matched and merged with the SHERPA parton shower based on Catani–Seymour dipole factorisation using the MEPS@NLO prescription. Samples were generated using the NNPDF3.0_{NNLO} PDF set, along with the dedicated set of tuned parton-shower parameters developed by the SHERPA authors.

The generated background MC samples were processed by the full ATLAS detector simulation based on GEANT4 [55]. The effect of multiple interactions in the same and neighbouring bunch

² The h_{damp} parameter is a resummation damping factor and one of the parameters that controls the matching of POWHEG matrix elements to the parton shower and thus effectively regulates the high- p_T radiation against which the $t\bar{t}$ system recoils.

crossings (pile-up) was modelled by overlaying the simulated hard-scattering event with inelastic pp events generated with PYTHIA 8.186 [56] using the NNPDF2.3LO set of PDF and the A3 set of tuned parameters [57]. Simulated events were reweighted to match the pile-up conditions in the data. All simulated events were processed using the same reconstruction algorithms and triggering requirements as used in data.

4 Event Reconstruction and Pre-selection

Proton-proton interaction vertices are reconstructed in events with at least two tracks, each with $p_T > 0.5$ GeV. The primary hard-scatter vertex is defined as the one with the largest value of the sum of squared track transverse momenta.

Muons are identified by matching tracks reconstructed in the MS to tracks reconstructed in the ID (referred to as combined muons). To increase the muon reconstruction efficiency, non-combined muon identification algorithms are also used in the analysis, including using the MS stand-alone tracks in the region $2.5 < |\eta| < 2.7$, and matching the ID tracks with calorimeter hit information within $|\eta| < 0.1$, as well as using the ID tracks associated with at least one local track segment in the MS. In the 4μ event selection at most one of the selected muons can be a non-combined muon. Each muon is then required to satisfy the ‘loose’ identification criteria [58]. Muons are required to be isolated using a particle-flow algorithm [59] and associated with the primary hard-scatter vertex by satisfying $|\frac{d_0}{\sigma_{d_0}}| < 3$ and $|z_0 \times \sin \theta| < 0.5$ mm, where d_0 is the transverse impact parameter calculated with respect to the measured beam-line position, σ_{d_0} its uncertainty, and z_0 is the longitudinal distance between the point at which d_0 is measured and the primary vertex. The minimum muon p_T threshold is 3 GeV.

In addition to muons, electrons, jets and missing transverse momentum (E_T^{miss}) are also used to select control samples for background estimation in this analysis. The reconstructions of these objects are described below.

Electrons are identified with a likelihood discriminator built from the shower shapes of electron energy deposits in the calorimeter, track-cluster matching, and some of the track quality distributions. Each electron is required to satisfy the ‘medium’ likelihood identification criteria [60], as well as similar vertex and isolation requirements as muons. The electrons are reconstructed in the region $|\eta| < 2.5$, excluding the transition area between the barrel and endcap calorimeters, $1.37 < |\eta| < 1.52$, and required to have $p_T > 7$ GeV.

Jets are reconstructed with the anti- k_t algorithm [61, 62] with a radius parameter of $R = 0.4$. The jet clustering input objects are based on particle-flow [59] in the ID and the calorimeter. Jets are required to have $p_T > 20$ GeV and $|\eta| < 2.5$. Jets containing B hadrons, referred to as b -jets, are identified with a multivariate discriminant [63]. To reduce the effect of pile-up, an additional quality requirement based on the ‘Jet-Vertex-Tagger’ algorithm (JVT) [64] is applied in jet identification.

E_T^{miss} is determined as the magnitude of the negative vectorial sum of the transverse momenta of the selected and calibrated physics objects (including muons, electrons, photons, and jets including hadronically decaying tau-leptons) and the ID tracks coming from the main vertex and not associated with any physics object (soft term) [65].

Events containing at least four muons with kinematics consistent with $Z(Z^*/\gamma^*) \rightarrow 4\mu$ production are then selected as follows. The four leading p_T -ordered muons are required to pass the p_T thresholds of 20, 15, 8, and 3 GeV, respectively. If a muon is selected as a non-combined muon, its p_T must be greater than 15 GeV. Any di-muon pair in the event must have an invariant mass $m_{\mu\mu}$ greater than 4 GeV and an angular separation ΔR larger than 0.2. To search for the $Z' \rightarrow \mu^+\mu^-$ signature, two muon pairs are selected based on their invariant mass values. The first pair (referred to as Z_1) is selected from all the possible $\mu^+\mu^-$ pairs to have the smallest mass difference between the Z_1 mass and the Z mass, $|m_Z - m_{Z_1}|$. The second $\mu^+\mu^-$ pair is selected from the remaining muons that has the highest invariant mass (referred to as Z_2). The correct signal di-muon pairing fraction varies with the Z' mass, where the selected di-muon pair that forms m_{Z_1} or m_{Z_2} originates from the Z' . For example, for $m_{Z'} = 5, 42, 63, 72,$ and 81 GeV, the correct di-muon pairing fractions are about 78%, 50%, 88%, 82%, and 90%, respectively. Finally, the selected four muons must have an invariant mass in a range of 80 to 180 GeV, but excluding the Higgs boson resonance mass region of 110 to 130 GeV. Including the 4μ events in the 4μ mass region between 130 to 180 GeV improves the Z' signal detection efficiency for its mass greater than 60 GeV.

The Z' signal efficiency at various stages of the event selection is shown in Table 2 for five representative mass points. The event selection efficiencies vary significantly depending on the Z' mass. At generator level, an MC filter is applied, which requires at least four muons with $p_T > 2$ GeV and $|\eta| < 3.0$. The MC filter efficiencies of these representative Z' signal samples are listed in the table as well.

Table 2: The Z' signal event selection efficiencies compared to the events passing the previous cut level for several representative mass points. The overall signal efficiencies are the products of the 4μ MC filter and the combined event selection efficiencies.

$m_{Z'}$ [GeV]	5	42	63	72	81
MC filter efficiency	32.8%	57.7%	61.0%	65.3%	70.0%
Number of identified muons ≥ 4	47.3%	74.1%	70.8%	72.4%	75.4%
$p_T^i (i = 1, 4) > 20, 15, 8, 3$ GeV	60.0%	82.6%	90.3%	93.6%	98.2%
$\Delta R(\mu_i, \mu_j) > 0.2$ & vertex requirement	87.2%	95.4%	96.2%	96.6%	97.2%
Isolation	54.2%	76.9%	79.2%	84.1%	87.5%
$m_{4\mu}$ within [80, 110] or [130, 180] GeV	91.9%	88.8%	58.9%	33.5%	16.8%
Combined event selection efficiency	12.3%	39.9%	28.7%	18.4%	10.6%
Overall 4μ signal efficiency	4.1%	23.0%	17.5%	11.9%	7.4%

The Z' production signature is searched for in the Z_1 or Z_2 mass spectrum depending on the

assumed Z' mass. The relatively high-mass Z' signals mostly appear as a peak in the Z_1 spectrum while the relatively low-mass signals mostly appear as a peak in the Z_2 spectrum. Representative examples of the predicted signal over background, after further selection with a deep learning approach which will be described in Section 6, are shown in Figure 4. In the analysis the Z_1 and Z_2 mass spectra are scanned to search for a Z' with mass greater or smaller than 42 GeV, respectively. The boundary value of 42 GeV is chosen based on the studies to optimize the search sensitivity.

The numbers of 4μ events in data and the estimated background yields are given in Table 3. More details about the estimation of the reducible backgrounds containing non-prompt muons can be found in Section 5. The total uncertainties of simulated backgrounds are also listed in the table. The evaluations of systematic uncertainties will be described in Section 7.

Table 3: The selected 4μ events in data and the estimated backgrounds and their combined statistical and systematic uncertainties.

Data	Total background	$qq \rightarrow ZZ^*$ from MC	$gg \rightarrow ZZ^*$ from MC	$ttV + VVV + H$ from MC	Reducible background from data
1131	1148 ± 70	1065^{+70}_{-69}	15.6 ± 2.5	6.2 ± 2.9	$61.1^{+8.3}_{-9.1}$

5 Estimation of Reducible Background from Data

A data-driven technique is used to estimate the reducible background from $Z + \text{jets}$ and $t\bar{t}$ production. Events from these processes may contain two prompt leptons from W or Z boson decays, together with additional activity such as heavy-flavor jets or misidentified components of jets yielding reconstructed muons, collectively referred to as non-prompt muons. Such backgrounds are estimated from data using a control sample of $\mu^+\mu^-\mu_j\mu_j$ events, selected with the standard signal requirements except that non-prompt muons, μ_j , are selected in place of two of the signal muons. Non-prompt muons are defined as muon candidates using the standard selection but fail the requirements on isolation and impact parameter. However, they are required to pass a much looser impact parameter significance requirement, $|\frac{d_0}{\sigma_{d_0}}| < 10$. The background in the signal sample is estimated by scaling each event in the selected $\mu^+\mu^-\mu_j\mu_j$ control sample by $f_1 \times f_2$, where the $f_i (i = 1, 2)$ is referred to as a "fake-factor" for each of the two non-prompt muons and is computed as a function of their p_T and $|\eta|$.

The fake-factor f is derived from two independent non-prompt muon enriched data control samples dominated by $Z + \text{jets}$ or $t\bar{t}$ events. The $Z + \text{jets}$ ($t\bar{t}$) sample contains non-prompt muons dominantly from light jets (heavy-flavor jets). The $Z + \text{jets}$ sample is tagged by two isolated prompt leptons from Z decays ($Z \rightarrow \mu^+\mu^-, e^+e^-$). The p_T -threshold for the two prompt leptons are 27 and 25 GeV and their invariant mass must be within 10 GeV of the Z mass. The E_T^{miss} of the event must be less than 25 GeV. The $t\bar{t}$ sample is tagged by two prompt isolated high- p_T $e^\pm\mu^\mp$ leptons with p_T thresholds of 28 and 25 GeV and associated with at least one b -jet. The

event is required to have $E_T^{\text{miss}} > 50$ GeV. If there is an additional isolated high- p_T lepton in the event, the transverse mass calculated with the E_T^{miss} and the third lepton is required to be less than 60 GeV to reduce the contribution from the $t\bar{t}W$ events.

Events with four muons that satisfy the signal selection criteria are removed from both $Z + \text{jets}$ and $t\bar{t}$ control samples. In addition, MC simulated diboson events satisfying the selection criteria are subtracted from these control samples. Excluding the target leptons, the additional reconstructed muon objects, passing either the signal muon or the non-prompt muon selection criteria are counted in the control samples. The fake-factor f is calculated as the ratio of the probability for a non-prompt muon to satisfy the signal muon selection criteria to the probability for a non-prompt muon to fail the signal muon selection. The factor f is derived as a function of $|\eta|$ and p_T of the non-prompt muons, which varies from 0.11 to 0.76 (0.01 to 0.27) in the $Z + \text{jets}$ ($t\bar{t}$) control sample. Then, the fake-factors derived from two data control samples are combined using the m_{Z1} spectra obtained from simulated 4μ background events from $Z + \text{jets}$ and $t\bar{t}$ processes. A simultaneous fit of the m_{Z1} spectra of the MC events to data selected in the $\mu^+\mu^-\mu_j\mu_j$ control sample is performed to determine the fractions of the $Z + \text{jets}$ and $t\bar{t}$ events in each bin of the mass spectrum.

The overall systematic uncertainty of f is about 14%. It is determined with alternative non-prompt muon selections, such as changing the muon isolation criteria in data control samples (7.6%), and the uncertainties of the $Z + \text{jets}$ and $t\bar{t}$ event fractions when combining the fake-factors derived from two control samples (8.6%). The statistical uncertainties of the control samples are also accounted as part of the systematic uncertainties (6.1%).

Additional reducible background contributions come from the WZ process. These events contain three prompt muons from W and Z decays and one non-prompt muon. This background is estimated by scaling a simulated $3\mu + \mu_j$ sample with the f derived from the $Z + \text{jets}$ sample.

The total estimated number of reducible background events is $61.1^{+8.3}_{-9.1}$ (with 88% and 12% contributions from the $\mu^+\mu^-\mu_j\mu_j$ and $3\mu + \mu_j$ control samples, respectively) as listed in Table 3.

6 Event Classification with Deep Learning Approach

The selected 4μ events are classified with a "Deep Learning" approach to further separate the Z' signal from the SM background. A parametrized deep neural network (pDNN) architecture [66] is used in the analysis. This algorithm allows the training of a single classifier for multiple signal mass hypotheses in the search range. In practice, the kinematic inputs together with the Z' mass parameters of signal and background are used for training. The MC generated Z' masses (listed in Table 1) are used as the multiple signal mass parameters, while the distribution of the mass parameter for background events is randomly drawn from the same distribution as for the signal class. The algorithm was implemented in the Keras [67] framework with the TensorFlow [68] backend. Two classifiers are trained for low (high) Z' mass searches using MC mass parameters lower (higher) than 40 GeV. During the training of the classifier, the training samples were composed of simulated signal and background 4μ events using the pre-selection described in

Section 4. A set of kinematic distributions were used for pDNN training input features. They are the p_T and η of each muon, the p_T of the Z_1 and Z_2 , the mass difference of the Z_1 and Z_2 , ΔR and $\Delta\eta$ of each muon pair that forms the Z_1 and Z_2 , and the p_T and mass of the 4μ system. Examples of the input variable distributions, both for representative signals ($m_{Z'} = 15$, and 51 GeV) and background, are shown in Figure 2 to compare the predicted and observed transverse momenta ($p_T^{Z_1}$ and $p_T^{Z_2}$) distributions and the mass difference of the Z_1 and Z_2 . In addition to the major background from the SM $Z(Z^*) \rightarrow 4\mu$ production, other backgrounds, including 4μ events containing non-prompt muons estimated from data, and from $t\bar{t}V$, VVV , and Higgs boson production processes, are included in the plots.

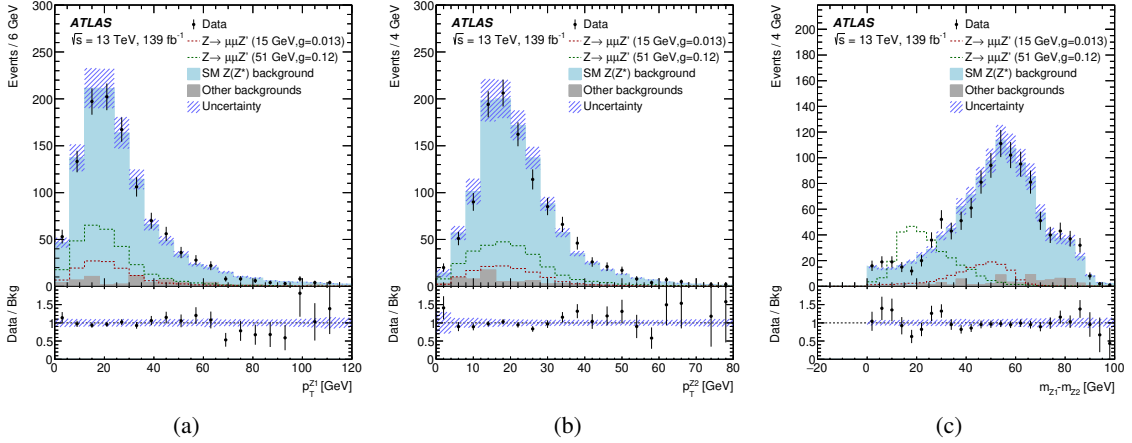


Figure 2: Distributions of $p_T^{Z_1}$ (a), and $p_T^{Z_2}$ (b), and the mass difference of the Z_1 and Z_2 candidates (c). Small background contributions are denoted as "other backgrounds", including 4μ events containing non-prompt muons estimated from data and from $t\bar{t}V$, VVV , and Higgs boson production processes.

The training fits the weight parameters of the pDNN models which are then applied to real data or MC samples to obtain the pDNN output discriminating variable. The m_{Z_1} or m_{Z_2} are used as the mass parameter when applying the model to data.

To improve the power of the pDNN classifier, the model is optimized through an automatic process developed with the package TUNE [69] and HEBO SEARCH algorithm [70]. The neural-network structure was chosen to have two fully connected hidden layers, each with 256 (32) nodes for the high (low) mass search in the analysis. Other training hyper-parameters, such as the *learning rate* with *decay* and *class weight*, for both high and low mass searches were also selected. Two pDNN output discriminant classifiers for high and low mass searches were obtained and are shown in Figure 3 for data and simulated signal and background events.

To maximize the search sensitivity, a scan of the pDNN output scores was performed to find the optimal cut values for each Z' mass hypothesis. These cut values vary from 0.42 to 0.74 (0.12 to 0.16) for the low (high) mass region. These cuts keep high signal efficiencies between 98% and 95% (90% and 50%), while the corresponding background reductions range from 10% to 50% (50% to 96%) for the low (high) mass region.

After the 4μ event selection with the pDNN classifier, the final discriminant to search for the Z' resonance signature is the Z_1 (for $m_{Z'} \geq 42$ GeV) or Z_2 (for $m_{Z'} \leq 42$ GeV) mass spectrum as shown in Figure 4. Data are compared to the estimated background together with two representative signals with masses of 15 and 51 GeV, shown in Figure 4(a) and 4(b), respectively. The values of the gauge coupling strengths (g) for the two mass points are chosen for the purpose of illustration.

One should note that the dimuon masses (m_{Z_1} , m_{Z_2}) are not used as the pDNN training variables, therefore cutting on the pDNN output scores does not sculpt the dimuon invariant mass distributions of the backgrounds (see Figure 4). To interpret the observed mass spectra, systematic uncertainties in the predictions are estimated in Section 7.

7 Systematic Uncertainties

Systematic uncertainties in the simulated event yields and shapes, for both signal and background processes, may arise from the calibration of the physics objects and from uncertainties in theoretical modelling used in the predictions.

The major experimental uncertainties come from the muon reconstruction, identification, and isolation requirement efficiencies. These efficiencies are corrected based on studies performed in data control regions. The energy and momentum scales and resolutions of the simulated objects are corrected to reproduce data from $Z \rightarrow \mu^+\mu^-$ and $J/\psi \rightarrow \mu^+\mu^-$ decays [58]. The uncertainties on the SM 4μ detection efficiency are determined by varying the nominal calibrations in the

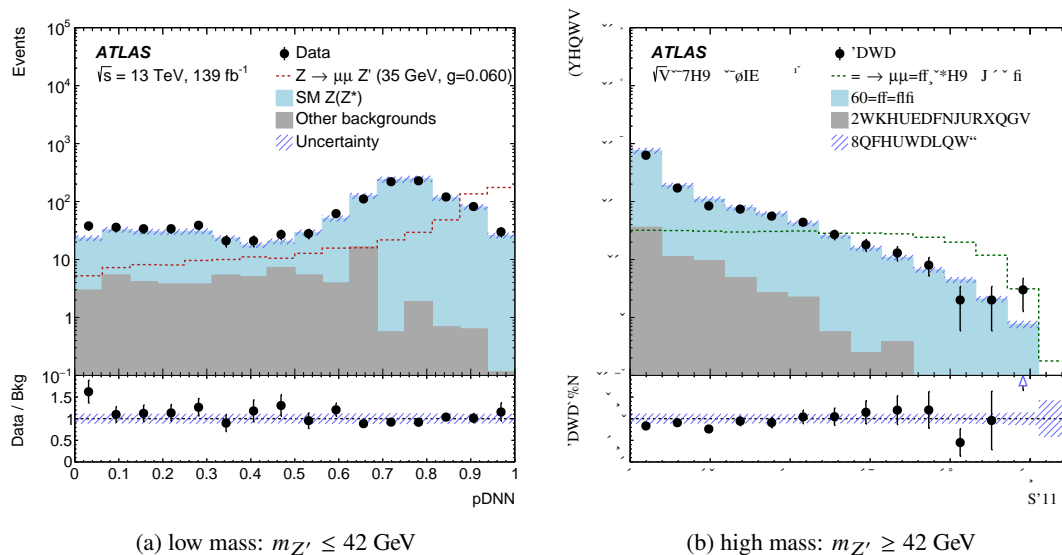


Figure 3: The pDNN output discriminant variable distributions for low mass (a) and high mass (b) with a signal sample at 35 GeV and 51 GeV, respectively.

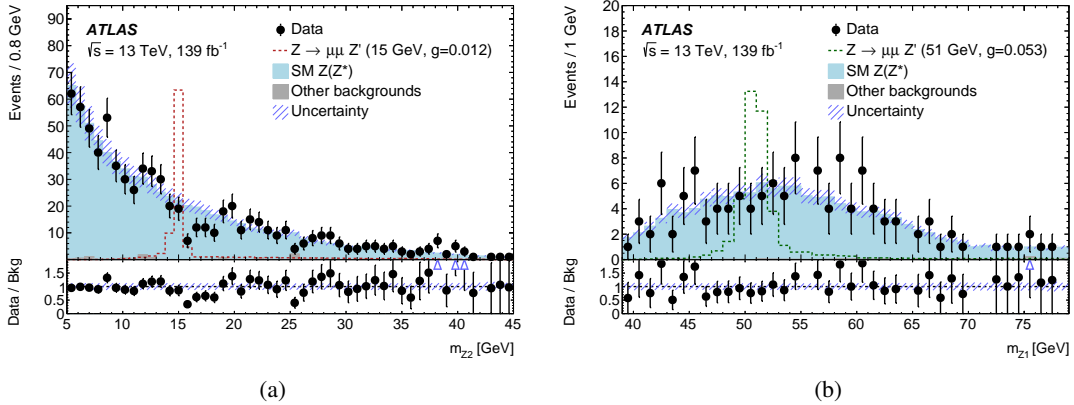


Figure 4: Mass spectra of m_{Z2} (left) and m_{Z1} (right) for the pDNN-selected events with a signal sample at 15 GeV and 51 GeV, respectively.

MC samples by one standard deviation, including muon momentum resolutions and scales, and the trigger, reconstruction, identification, and isolation requirement efficiencies. The overall relative experimental uncertainties in the SM 4μ background event selection efficiency is about 3.9%, dominated by the uncertainty of the isolation efficiency (2.9%) and the low p_T calibration uncertainty (2.0%). The hypothetical Z' signal event selection efficiency uncertainties vary from 8.3% to 3.9%, depending on the Z' mass. In addition, the uncertainty in the combined 2015–2018 integrated luminosity is 1.7% [71], obtained using the LUCID-2 detector [72] for the primary luminosity measurements.

Sources of theoretical uncertainties come from the choice of QCD scales (renormalization μ_R and factorization μ_F), strong coupling constant α_S , and PDFs, as well as the parton shower models. These uncertainties affect the signal and background event selection efficiencies, normalization, and the shape of their kinematic distributions. The scales are varied independently from 0.5 to 2.0 times the nominal values and the largest deviation is chosen as the systematic uncertainty. The PDF uncertainty is estimated by comparing events generated with different PDF sets, as well as the uncertainties from the nominal PDF set itself. The maximal variation (envelope) is accounted for as the systematic uncertainty, following the PDF4LHC [73] recommendations. The α_S uncertainty is estimated by comparing events generated with different α_S values using the nominal PDF set. The parton shower uncertainty is estimated by comparing events with different parton shower parameters in the Sherpa MC samples. For the $Z(Z^*) \rightarrow 4\mu$ process, the relative uncertainties of event yields for scale, PDF, α_S , and parton shower, are 4.6%, 1.8%, 1.0%, and 1.9%, respectively. The uncertainties of small background contributions from the $t\bar{t}V$ (5.2 ± 0.7), VVV (0.5 ± 0.25), and Higgs boson (0.53 ± 0.06) processes are evaluated and included in the analysis.

The interference effect between the signal and background is estimated (using generator-level MC samples simulated with MADGRAPH5_aMC@NLO) by evaluating the cross-section ratio, $\Delta\sigma/\sigma_{Z'}$, where $\Delta\sigma$ is the difference of the cross-section from the inclusive MC sample and the sum of the

cross-sections of the signal and background samples in the Z' detection phase space. The effect varies from 1.8 to 7.5% for the Z' mass from 5 - 81 GeV, which is accounted for as additional signal yield systematic uncertainties. In addition, the MC Z' signal filter acceptance uncertainty is estimated to be about 2%, which is calculated by varying the QCD scales, the PDF-sets, and the strong coupling constant using MC events at the generator-level for different Z' mass points.

All the uncertainties (from both experiment and theory) on the final discriminant di-muon mass spectra are included as nuisance parameters in the signal extraction fitting process described in Section 8.1.

8 Data Interpretation and Results

The statistical analysis is performed by comparing the data to the sum of the background prediction and the signal to search for the Z' signature and information about the $pp \rightarrow \mu^+ \mu^- Z' \rightarrow 4\mu$ signal production cross-section and the associated coupling strength. In case of no significant data excess over the background prediction, upper limits on the signal production cross-section times the decay branching fraction for different Z' masses are set at 95% confidence level (CL).

8.1 Statistical Procedure and Results

The statistical procedure used to interpret the data is described in Ref. [74]. The likelihood function is constructed from the product of Poisson probabilities:

$$L(\text{data} | \mu, \theta) = \prod_{i=1}^N \text{Poisson}(\text{data}_i | \mu \cdot s_i(\theta) + b_i(\theta)) \times G(\tilde{\theta} | \theta)$$

where i is the bin-index of the fitted variable distribution; μ is the signal strength, and θ denotes the nuisance parameters, which represent the uncertainties of the measurements; $G(\tilde{\theta} | \theta)$ is the Gaussian scaling function of the nuisance parameters constructed as deviations from the nominal model of the systematic uncertainties, where $\tilde{\theta}$ provides a maximum likelihood estimate for θ . The parameter of interest in the statistical analysis is the global signal strength factor μ , which acts as a scale factor on the total number of events predicted by the signal model. This factor is defined such that $\mu = 0$ corresponds to the background-only hypothesis and $\mu > 0$ corresponds to a Z' signal in addition to the background. Hypothesised values of μ are tested based on the profile likelihood ratio [75], which compares data with background-only (b) and signal+background ($s + b$) models using the following test statistic:

$$q_\mu = \begin{cases} -2 \ln \frac{L(\text{data} | \mu, \hat{\theta}_\mu)}{L(\text{data} | \hat{\mu}, \hat{\theta})} & \hat{\mu} \leq \mu \\ 0 & \hat{\mu} > \mu \end{cases}$$

where $\hat{\mu}$ and $\hat{\theta}$ are the values for μ and θ when maximizing the L with all parameters floating, which are named as the unconditional maximum-likelihood (ML) estimators; $\hat{\theta}_\mu$ is the conditional

ML estimator of θ for a fixed value of μ . This test statistic extracts the information on the signal strength from a full likelihood fit to the data. The likelihood function includes all the parameters that describe the systematic uncertainties and their correlations.

The significance of an excess in the data is first quantified with the local p_0 , the probability that the background can produce a fluctuation greater than or equal to the excess observed in data. The equivalent formulation in terms of number of standard deviations is referred to as the local significance, which is computed from test statistic q_0 :

$$p_0 = \text{P}(q_0 < q_0^{obs}).$$

The global probability for the most significant excess to be observed anywhere in a given search region is estimated with the method described in Ref. [76].

In case of no significant data excess over the background, exclusion limits are set, based on the CLs prescription [77], which calculates the ratio of the probabilities based on the $s + b$ background-only models:

$$\text{CL}_s(\mu) = \frac{\text{CL}_{s+b}}{\text{CL}_b} = \frac{\text{P}(q_\mu > q_\mu^{obs})}{\text{P}(q_0 > q_0^{obs})}$$

A value of μ is regarded as excluded at 95% confident level when CLs is less than 5%.

The statistical tests are performed by first searching for data excesses by means of a p_0 scan, and in case no such significant data excess is found, by setting limits on the Z' production cross-section times the branching fraction. In both steps the values and reconstructed mass distributions of hypothesized Z' mass $m_{Z'}$ are used. The steps between the mass points used in these test procedures are set to match the mass resolutions determined by reconstruction of the di-muon invariant mass. A linear interpolation of the expected event yields and shapes between the MC generated signal samples is used in the fitting process. The asymptotic approximation [75] upon which the results are based has been validated against the method (detailed in Ref. [74]) of using pseudo-experiments for several mass points.

In both steps of the statistical tests, data are fit to the m_{Z1} and m_{Z2} spectrum with background (b) only and signal+background ($s + b$) hypotheses. In the fitting process each mass spectrum is divided in the signal region (SR) and the background control region (CR). For each Z' mass point the SR is defined in a mass window of $m_{Z'} \pm 3\sigma_{m_{\mu\mu}}$ of the di-muon mass spectrum. The sidebands outside of the SR are defined as the CR. The di-muon mass resolution $\sigma_{m_{\mu\mu}}$ is determined by the fully simulated Z' mass distribution, which combines the Z' natural width and the detector resolution, ranging from 0.10 to 1.75 GeV. The mass resolution is mostly dominated by the detector resolution. Finer binning is used in the SR to enhance the sensitivity. The background CR is used to constrain the overall normalization for the background in the signal region. The shape of the major background from $Z(Z^*) \rightarrow 4\mu$ is fixed with prior uncertainties included in the fitting process, but the normalization (or strength) floats in the fit. Other background normalizations and shapes are fixed with prior uncertainties included in the fitting.

8.2 The p_0 Scan Results

The p_0 -values corresponding to the background-only hypothesis are scanned in the mass range of this analysis. A binned profile-likelihood fit [75] is performed simultaneously across the Z' signal-region and the background control region using the predicted and observed mass spectrum as inputs. Data are fit to the m_{Z1} and m_{Z2} distributions for $m_{Z'} \geq 42$ GeV and $m_{Z'} \leq 42$ GeV, respectively, with a "sliding" mass window as the defined SR changes for different Z' mass points. The chosen bin-size inside the SR is around $0.3 \sigma_{m_{\mu\mu}}$, for each mass point. The total number of bins in the CR is 20. The fit mass range of m_{Z1} (m_{Z2}) is [30, 85] GeV ([0, 45] GeV).

The p_0 -values at different Z' mass hypothesis points are computed and transformed into Gaussian standard deviations to indicate the significance as shown in Figure 5. The smallest p_0 -value is at 39.6 GeV, corresponding to a local 2.65σ deviation from the background-only hypothesis, while the global deviation [76] is found to be 0.52σ , indicating that no significant data excess over the expected background is observed.

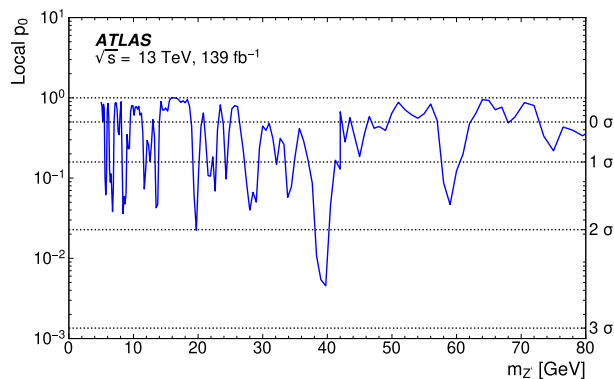


Figure 5: The p_0 -value scan across the Z' mass signal regions.

8.3 Upper Limits

The upper limits on the production cross-section times branching fraction of the $pp \rightarrow \mu^+ \mu^- Z' \rightarrow 4\mu$ process are calculated using a similar fitting procedure described in Section 8.2. Confidence intervals are computed based on the profile-likelihood-ratio test statistics [75]. The observed and expected upper limits at 95% CL on the cross-section times branching fraction, $\sigma(pp \rightarrow Z' \mu\mu \rightarrow 4\mu)$, are shown in Figure 6(a). The upper limits on the coupling parameter g are extracted from the limits of the Z' production cross-section times branching fraction using the $L_\mu - L_\tau$ model, which is determined by counting all the possible Z' decay modes in this model. At each generated Z' mass point, a limit on the coupling strength g has been obtained from the cross-section limit. The observed and expected upper limits on the coupling parameter g are shown in Figure 6(b). The limits on the coupling g are in the range of 0.003 (for $m_{Z'} = 5$ GeV) to 0.2 (for $m_{Z'} = 81$

GeV) depending on the Z' mass ranging from 5 to 81 GeV. This ensures that the ratio of the Z' natural width and mass, $\Gamma(Z')/m_{Z'}$, is well below 1% in this mass range.

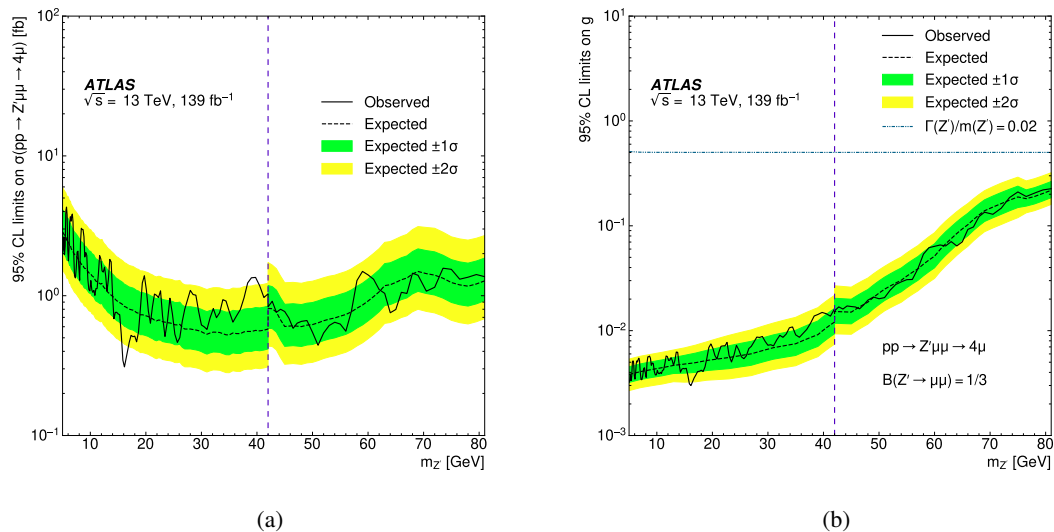


Figure 6: 95% CL upper limits (expected and observed) on the cross-sections times branching fraction (a) and coupling parameter (b). The discontinuity at 42 GeV represents the border of the low/high mass classifiers. Considering the dimuon mass resolution of 2% of the ATLAS detector, the horizontal dashed line in (b) indicates the upper limit on the valid coupling parameter of the model used in this analysis.

Motivated by theoretical interpretations in Ref. [11], a 2-dimensional exclusion contour at 95% CL in the parameter-space of $(m_{Z'}, g)$ of the $L_\mu - L_\tau$ model from this analysis is produced and shown in Figure 7. The parameter space exclusion regions calculated by theorists using data from the Neutrino Trident experiment [78] and the B_s mixing measurements by a global analysis performed in Ref. [11] are also shown in Figure 7. This had left a large gap in the parameter space not yet excluded. This gap is now largely excluded by this analysis.

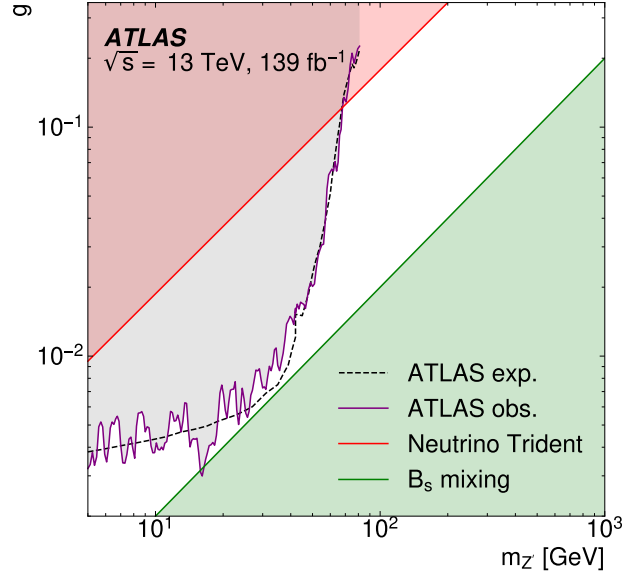


Figure 7: The coupling parameter g limits from this search as a function of the Z' mass compared to the limits [11] from the Neutrino Trident (red) and the B_s mixing (green) experimental results.

9 Conclusion

A search for a new vector gauge boson Z' predicted by the $L_\mu - L_\tau$ models has been performed with a 4μ final state in the invariant mass range of [80, 180] GeV, excluding the Higgs boson mass window [110, 130] GeV, using 139 fb^{-1} of $\sqrt{s} = 13 \text{ TeV}$ proton-proton collision data collected with the ATLAS detector. No significant excess of events over the expected SM background is observed. Therefore, upper limits are set on the Z' production cross-section times the decay branching fraction of the $pp \rightarrow Z' \mu^+ \mu^- \rightarrow \mu^+ \mu^- \mu^+ \mu^-$ process, varying from 0.31 to 4.3 fb at 95% CL, in a Z' mass range of [5, 81] GeV, from which the coupling strength g of the Z' to muons above 0.003 to 0.2 (depending on the Z' mass) are excluded in the same mass range. This search shows significant sensitivity improvements over previous indirect and direct searches of the Z' with 4μ final state. An interesting parameter space of the $L_\mu - L_\tau$ model prediction that was not excluded by previous experiments is now largely excluded by this search.

Acknowledgements

We thank CERN for the very successful operation of the LHC, as well as the support staff from our institutions without whom ATLAS could not be operated efficiently.

We acknowledge the support of ANPCyT, Argentina; YerPhI, Armenia; ARC, Australia; BMWFW and FWF, Austria; ANAS, Azerbaijan; SSTC, Belarus; CNPq and FAPESP, Brazil; NSERC, NRC and CFI, Canada; CERN; ANID, Chile; CAS, MOST and NSFC, China; Minciencias, Colombia; MEYS CR, Czech Republic; DNRF and DNSRC, Denmark; IN2P3-CNRS and CEA-DRF/IRFU, France; SRNSFG, Georgia; BMBF, HGF and MPG, Germany; GSRI, Greece; RGC and Hong Kong SAR, China; ISF and Benozziyo Center, Israel; INFN, Italy; MEXT and JSPS, Japan; CNRST, Morocco; NWO, Netherlands; RCN, Norway; MEiN, Poland; FCT, Portugal; MNE/IFA, Romania; JINR; MES of Russia and NRC KI, Russian Federation; MESTD, Serbia; MSSR, Slovakia; ARRS and MIZŠ, Slovenia; DSI/NRF, South Africa; MICINN, Spain; SRC and Wallenberg Foundation, Sweden; SERI, SNSF and Cantons of Bern and Geneva, Switzerland; MOST, Taiwan; TENMAK, Türkiye; STFC, United Kingdom; DOE and NSF, United States of America. In addition, individual groups and members have received support from BCKDF, CANARIE, Compute Canada and CRC, Canada; COST, ERC, ERDF, Horizon 2020 and Marie Skłodowska-Curie Actions, European Union; Investissements d’Avenir Labex, Investissements d’Avenir IDEX and ANR, France; DFG and AvH Foundation, Germany; Herakleitos, Thales and Aristeia programmes co-financed by EU-ESF and the Greek NSRF, Greece; BSF-NSF and GIF, Israel; Norwegian Financial Mechanism 2014-2021, Norway; NCN and NAWA, Poland; La Caixa Banking Foundation, CERCA Programme Generalitat de Catalunya and PROMETEO and GenT Programmes Generalitat Valenciana, Spain; Göran Gustafssons Stiftelse, Sweden; The Royal Society and Leverhulme Trust, United Kingdom.

The crucial computing support from all WLCG partners is acknowledged gratefully, in particular from CERN, the ATLAS Tier-1 facilities at TRIUMF (Canada), NDGF (Denmark, Norway, Sweden), CC-IN2P3 (France), KIT/GridKA (Germany), INFN-CNAF (Italy), NL-T1 (Netherlands), PIC (Spain), ASGC (Taiwan), RAL (UK) and BNL (USA), the Tier-2 facilities worldwide and large non-WLCG resource providers. Major contributors of computing resources are listed in Ref. [79].

References

- [1] ATLAS Collaboration, *The ATLAS Experiment at the CERN Large Hadron Collider*, [JINST **3** \(2008\) S08003](#).
- [2] X.-G. He, G. C. Joshi, H. Lew and R. R. Volkas, *Simplest Z' model*, [Phys. Rev. D **44** \(1991\) 2118](#).
- [3] Muon g-2 Collaboration, *Measurement of the Positive Muon Anomalous Magnetic Moment to 0.46 ppm*, [Phys. Rev. Lett. **126** \(2021\) 141801](#), arXiv: [2104.03281 \[hep-ex\]](#).
- [4] A. Keshavarzi, *The Muon g-2 experiment at Fermilab*, [EPJ Web of Conferences **212** \(2019\) 05003](#), ed. by M. Achasov, F. Ignatov and P. Krokovny.
- [5] G. Venanzoni, *The Fermilab Muon g-2 Experiment*, [PoS EPS-HEP2015 \(2016\) 568](#).
- [6] Muon g-2 Collaboration, *Final report of the E821 muon anomalous magnetic moment measurement at BNL*, [Phys. Rev. D **73** \(2006\) 072003](#).
- [7] LHCb Collaboration, *Test of lepton universality in beauty-quark decays*, [Nat. Phys. **18** \(2022\) 277](#).
- [8] LHCb Collaboration, *Measurement of Form-Factor-Independent Observables in the Decay $B^0 \rightarrow K^{*0} \mu^+ \mu^-$* , [Phys. Rev. Lett. **111** \(2013\) 191801](#).
- [9] LHCb Collaboration, *Test of lepton universality using $B^+ \rightarrow K^+ \ell^+ \ell^-$ decays*, [Phys. Rev. Lett. **113** \(2014\) 151601](#).
- [10] LHCb Collaboration, *Measurement of CP-Averaged Observables in the $B^0 \rightarrow K^{*0} \mu^+ \mu^-$ Decay*, [Phys. Rev. Lett. **125** \(2020\) 011802](#).
- [11] W. Altmannshofer, S. Gori, S. Profumo and F. S. Queiroz, *Explaining dark matter and B decay anomalies with an $L_\mu - L_\tau$ model*, [JHEP **12** \(2016\) 106](#), arXiv: [1609.04026 \[hep-ph\]](#).
- [12] E. Ma, D. Roy and S. Roy, *Gauged $L_\mu - L_\tau$ with large muon anomalous magnetic moment and the bimaximal mixing of neutrinos*, [Phys. Lett. B **525** \(2002\) 101](#).
- [13] P. Langacker, *The physics of heavy Z' gauge bosons*, [Rev. Mod. Phys. **81** \(2009\) 1199](#).
- [14] CMS Collaboration, *Observation of Z Decays to Four Leptons with the CMS Detector at the LHC*, [JHEP **12** \(2012\) 034](#), arXiv: [1210.3844 \[hep-ex\]](#).
- [15] ATLAS Collaboration, *Measurements of Four-Lepton Production at the Z Resonance in pp Collisions at $\sqrt{s} = 7$ and 8 TeV with ATLAS*, [Phys. Rev. Lett. **112** \(2014\) 231806](#), arXiv: [1403.5657 \[hep-ex\]](#).

- [16] CMS Collaboration, *Measurements of the $pp \rightarrow ZZ$ production cross section and the $Z \rightarrow 4\ell$ branching fraction, and constraints on anomalous triple gauge couplings at $\sqrt{s} = 13$ TeV*, *Eur. Phys. J. C* **78** (2018) 165, arXiv: [1709.08601 \[hep-ex\]](#),
Erratum: *Eur. Phys. J. C* **78.6** (2018) 515.
- [17] CMS Collaboration, *Search for an $L_\mu-L_\tau$ gauge boson using $Z \rightarrow 4\mu$ events in proton–proton collisions at $\sqrt{s} = 13$ TeV*, *Phys. Lett. B* **792** (2019) 345, arXiv: [1808.03684 \[hep-ex\]](#).
- [18] ATLAS Collaboration, *ATLAS Insertable B-Layer: Technical Design Report*, ATLAS-TDR-19; CERN-LHCC-2010-013, 2010, URL: <https://cds.cern.ch/record/1291633>, Addendum: ATLAS-TDR-19-ADD-1; CERN-LHCC-2012-009, 2012, URL: <https://cds.cern.ch/record/1451888>.
- [19] B. Abbott et al., *Production and integration of the ATLAS Insertable B-Layer*, *JINST* **13** (2018) T05008, arXiv: [1803.00844 \[physics.ins-det\]](#).
- [20] ATLAS Collaboration, *Performance of the ATLAS trigger system in 2015*, *Eur. Phys. J. C* **77** (2017) 317, arXiv: [1611.09661 \[hep-ex\]](#).
- [21] ATLAS Collaboration, *The ATLAS Collaboration Software and Firmware*, ATL-SOFT-PUB-2021-001, 2021, URL: <https://cds.cern.ch/record/2767187>.
- [22] ATLAS Collaboration, *ATLAS data quality operations and performance for 2015-2018 data-taking*, *JINST* **15** (2020) P04003.
- [23] ATLAS Collaboration, *Performance of the ATLAS muon triggers in Run 2*, *JINST* **15** (2020) P09015, arXiv: [2004.13447 \[hep-ex\]](#).
- [24] F. del Aguila, M. Chala, J. Santiago and Y. Yamamoto, *Collider limits on leptophilic interactions*, *JHEP* **03** (2015) 059, arXiv: [1411.7394](#).
- [25] J. Alwall et al., *The automated computation of tree-level and next-to-leading order differential cross sections, and their matching to parton shower simulations*, *JHEP* **07** (2014) 079, arXiv: [1405.0301 \[hep-ph\]](#).
- [26] C. Degrande et al., *UFO - The Universal FeynRules Output*, *Comput. Phys. Commun.* **183** (2012) 1201, arXiv: [1108.2040 \[hep-ph\]](#).
- [27] A. Alloul, N. D. Christensen, C. Degrande, C. Duhr and B. Fuks, *FeynRules 2.0 - A complete toolbox for tree-level phenomenology*, *Comput. Phys. Commun.* **185** (2014) 2250, arXiv: [1310.1921 \[hep-ph\]](#).
- [28] M. Grazzini, S. Kallweit and D. Rathlev, *ZZ production at the LHC: Fiducial cross sections and distributions in NNLO QCD*, *Phys. Lett. B* **750** (2015) 407.
- [29] A. H. Ajjath et al., *Resummed Drell-Yan cross-section at N^3LL* , *JHEP* **10** (2020) 153.
- [30] R. D. Ball et al., *Parton distributions with LHC data*, *Nucl. Phys. B* **867** (2013) 244, arXiv: [1207.1303 \[hep-ph\]](#).

- [31] P. Golonka and Z. Was,
PHOTOS Monte Carlo: a precision tool for QED corrections in Z and W decays,
Eur. Phys. J. C **45** (2006) 97, arXiv: [hep-ph/0506026](#).
- [32] N. Davidson, T. Przedzinski and Z. Was,
PHOTOS Interface in C++: Technical and physics documentation,
Comput. Phys. Commun. **199** (2016) 86, arXiv: [1011.0937 \[hep-ph\]](#).
- [33] ATLAS Collaboration, *The ATLAS Simulation Infrastructure*,
Eur. Phys. J. C **70** (2010) 823, arXiv: [1005.4568 \[physics.ins-det\]](#).
- [34] E. Bothmann et al., *Event generation with Sherpa 2.2*, *SciPost Phys.* **7** (2019) 034,
arXiv: [1905.09127 \[hep-ph\]](#).
- [35] T. Gleisberg and S. Höche, *Comix, a new matrix element generator*, *JHEP* **12** (2008) 039,
arXiv: [0808.3674 \[hep-ph\]](#).
- [36] S. Schumann and F. Krauss,
A parton shower algorithm based on Catani–Seymour dipole factorisation,
JHEP **03** (2008) 038, arXiv: [0709.1027 \[hep-ph\]](#).
- [37] S. Höche, F. Krauss, M. Schönherr and F. Siegert,
A critical appraisal of NLO+PS matching methods, *JHEP* **09** (2012) 049,
arXiv: [1111.1220 \[hep-ph\]](#).
- [38] S. Höche, F. Krauss, M. Schönherr and F. Siegert,
QCD matrix elements + parton showers. The NLO case, *JHEP* **04** (2013) 027,
arXiv: [1207.5030 \[hep-ph\]](#).
- [39] S. Catani, F. Krauss, R. Kuhn and B. R. Webber, *QCD Matrix Elements + Parton Showers*,
JHEP **11** (2001) 063, arXiv: [hep-ph/0109231](#).
- [40] S. Höche, F. Krauss, S. Schumann and F. Siegert,
QCD matrix elements and truncated showers, *JHEP* **05** (2009) 053,
arXiv: [0903.1219 \[hep-ph\]](#).
- [41] F. Buccioni et al., *OpenLoops 2*, *Eur. Phys. J. C* **79** (2019) 866,
arXiv: [1907.13071 \[hep-ph\]](#).
- [42] F. Cascioli, P. Maierhofer and S. Pozzorini, *Scattering Amplitudes with Open Loops*,
Phys. Rev. Lett. **108** (2012) 111601, arXiv: [1111.5206 \[hep-ph\]](#).
- [43] A. Denner, S. Dittmaier and L. Hofer,
COLLIER: A fortran-based complex one-loop library in extended regularizations,
Comput. Phys. Commun. **212** (2017) 220, arXiv: [1604.06792 \[hep-ph\]](#).
- [44] R. D. Ball et al., *Parton distributions for the LHC run II*, *JHEP* **04** (2015) 040,
arXiv: [1410.8849 \[hep-ph\]](#).
- [45] S. Frixione, P. Nason and G. Ridolfi,
A positive-weight next-to-leading-order Monte Carlo for heavy flavour hadroproduction,
JHEP **09** (2007) 126, arXiv: [0707.3088 \[hep-ph\]](#).

- [46] P. Nason, *A new method for combining NLO QCD with shower Monte Carlo algorithms*, *JHEP* **11** (2004) 040, arXiv: [hep-ph/0409146](#).
- [47] S. Frixione, P. Nason and C. Oleari, *Matching NLO QCD computations with parton shower simulations: the POWHEG method*, *JHEP* **11** (2007) 070, arXiv: [0709.2092 \[hep-ph\]](#).
- [48] S. Alioli, P. Nason, C. Oleari and E. Re, *A general framework for implementing NLO calculations in shower Monte Carlo programs: the POWHEG BOX*, *JHEP* **06** (2010) 043, arXiv: [1002.2581 \[hep-ph\]](#).
- [49] ATLAS Collaboration, *Studies on top-quark Monte Carlo modelling for Top2016*, ATL-PHYS-PUB-2016-020, 2016, URL: <https://cds.cern.ch/record/2216168>.
- [50] T. Sjöstrand et al., *An introduction to PYTHIA 8.2*, *Comput. Phys. Commun.* **191** (2015) 159, arXiv: [1410.3012 \[hep-ph\]](#).
- [51] ATLAS Collaboration, *ATLAS Pythia 8 tunes to 7 TeV data*, ATL-PHYS-PUB-2014-021, 2014, URL: <https://cds.cern.ch/record/1966419>.
- [52] E. Re, *Single-top Wt -channel production matched with parton showers using the POWHEG method*, *Eur. Phys. J. C* **71** (2011) 1547, arXiv: [1009.2450 \[hep-ph\]](#).
- [53] S. Frixione, E. Laenen, P. Motylinski, C. White and B. R. Webber, *Single-top hadroproduction in association with a W boson*, *JHEP* **07** (2008) 029, arXiv: [0805.3067 \[hep-ph\]](#).
- [54] C. Anastasiou, L. J. Dixon, K. Melnikov and F. Petriello, *High precision QCD at hadron colliders: Electroweak gauge boson rapidity distributions at next-to-next-to leading order*, *Phys. Rev. D* **69** (2004) 094008, arXiv: [hep-ph/0312266](#).
- [55] S. Agostinelli et al., *GEANT4 – a simulation toolkit*, *Nucl. Instrum. Meth. A* **506** (2003) 250.
- [56] T. Sjöstrand, S. Mrenna and P. Z. Skands, *A brief introduction to PYTHIA 8.1*, *Comput. Phys. Commun.* **178** (2008) 852, arXiv: [0710.3820 \[hep-ph\]](#).
- [57] ATLAS Collaboration, *The Pythia 8 A3 tune description of ATLAS minimum bias and inelastic measurements incorporating the Donnachie–Landshoff diffractive model*, ATL-PHYS-PUB-2016-017, 2016, URL: <https://cds.cern.ch/record/2206965>.
- [58] ATLAS Collaboration, *Muon reconstruction and identification efficiency in ATLAS using the full Run 2 pp collision data set at $\sqrt{s} = 13$ TeV*, *Eur. Phys. J. C* **81** (2021) 578, arXiv: [2012.00578 \[hep-ex\]](#).
- [59] ATLAS Collaboration, *Jet reconstruction and performance using particle flow with the ATLAS Detector*, *Eur. Phys. J. C* **77** (2017) 466, arXiv: [1703.10485 \[hep-ex\]](#).
- [60] ATLAS Collaboration, *Electron and photon performance measurements with the ATLAS detector using the 2015–2017 LHC proton-proton collision data*, *JINST* **14** (2019) P12006.

- [61] ATLAS Collaboration, *Track assisted techniques for jet substructure*, ATL-PHYS-PUB-2018-012, 2018, URL: <https://cds.cern.ch/record/2630864>.
- [62] M. Cacciari, G. P. Salam and G. Soyez, *FastJet user manual*, *Eur. Phys. J. C* **72** (2012) 1896, arXiv: 1111.6097 [hep-ph].
- [63] ATLAS Collaboration, *Optimisation of the ATLAS b-tagging performance for the 2016 LHC Run*, ATL-PHYS-PUB-2016-012, 2016, URL: <https://cds.cern.ch/record/2160731>.
- [64] ATLAS Collaboration, *Tagging and suppression of pileup jets with the ATLAS detector*, ATLAS-CONF-2014-018, 2014, URL: <https://cds.cern.ch/record/1700870>.
- [65] ATLAS Collaboration, *Performance of missing transverse momentum reconstruction with the ATLAS detector using proton–proton collisions at $\sqrt{s} = 13$ TeV*, *Eur. Phys. J. C* **78** (2018) 903, arXiv: 1802.08168 [hep-ex].
- [66] P. Baldi, K. Cranmer, T. Faucett, P. Sadowski and D. Whiteson, *Parameterized neural networks for high-energy physics*, *Eur. Phys. J. C* **76** (2016).
- [67] F. Chollet et al., *Keras*, <https://keras.io>, 2015.
- [68] Mart'in Abadi et al., *TensorFlow: Large-Scale Machine Learning on Heterogeneous Systems*, Software available from tensorflow.org, 2015, URL: <https://www.tensorflow.org/>.
- [69] R. Liaw et al., *Tune: A Research Platform for Distributed Model Selection and Training*, (2018), arXiv: 1807.05118 [cs.LG].
- [70] A. I. Cowen-Rivers et al., *HEBO Pushing The Limits of Sample-Efficient Hyperparameter Optimisation*, 2020, arXiv: 2012.03826 [cs.LG].
- [71] ATLAS Collaboration, *Luminosity determination in pp collisions at $\sqrt{s} = 13$ TeV using the ATLAS detector at the LHC*, ATLAS-CONF-2019-021, 2019, URL: <https://cds.cern.ch/record/2677054>.
- [72] G. Avoni et al., *The new LUCID-2 detector for luminosity measurement and monitoring in ATLAS*, *JINST* **13** (2018) P07017.
- [73] J. Butterworth et al., *PDF4LHC recommendations for LHC Run II*, *J. Phys. G* **43** (2016) 023001, arXiv: 1510.03865 [hep-ph].
- [74] ATLAS Collaboration, *Combined search for the Standard Model Higgs boson in pp collisions at $\sqrt{s} = 7$ TeV with the ATLAS detector*, *Phys. Rev. D* **86** (2012) 032003, arXiv: 1207.0319 [hep-ex].
- [75] G. Cowan, K. Cranmer, E. Gross and O. Vitells, *Asymptotic formulae for likelihood-based tests of new physics*, *Eur. Phys. J. C* **71** (2011) 1554, arXiv: 1007.1727 [physics.data-an], Erratum: *Eur. Phys. J. C* **73** (2013) 2501.

- [76] E. Gross and O. Vitells, *Trial factors for the look elsewhere effect in high energy physics*, [Eur. Phys. J. C **70** \(2010\) 525](#).
- [77] A. L. Read, *Presentation of search results: the CL_S technique*, [J. Phys. G **28** \(2002\) 2693](#).
- [78] S. R. Mishra et al., *Neutrino tridents and W-Z interference*, [Phys. Rev. Lett. **66** \(24 1991\) 3117](#).
- [79] ATLAS Collaboration, *ATLAS Computing Acknowledgements*, ATL-SOFT-PUB-2021-003, URL: <https://cds.cern.ch/record/2776662>.

The ATLAS Collaboration

G. Aad¹⁰¹, B. Abbott¹¹⁹, D.C. Abbott¹⁰², K. Abeling⁵⁵, S.H. Abidi²⁹, A. Abouhorma^{35e},
H. Abramowicz¹⁵⁰, H. Abreu¹⁴⁹, Y. Abulaiti¹¹⁶, A.C. Abusleme Hoffman^{136a},
B.S. Acharya^{68a,68b,p}, B. Achkar⁵⁵, C. Adam Bourdarios⁴, L. Adamczyk^{84a}, L. Adamek¹⁵⁴,
S.V. Addepalli²⁶, J. Adelman¹¹⁴, A. Adiguzel^{21c}, S. Adorni⁵⁶, T. Adye¹³³, A.A. Affolder¹³⁵,
Y. Afik³⁶, M.N. Agaras¹³, J. Agarwala^{72a,72b}, A. Aggarwal⁹⁹, C. Agheorghiesei^{27c},
J.A. Aguilar-Saavedra^{129f}, A. Ahmad³⁶, F. Ahmadov^{38,aa}, W.S. Ahmed¹⁰³, S. Ahuja⁹⁴, X. Ai⁴⁸,
G. Aielli^{75a,75b}, I. Aizenberg¹⁶⁸, M. Akbiyik⁹⁹, T.P.A. Åkesson⁹⁷, A.V. Akimov³⁷,
K. Al Khoury⁴¹, G.L. Alberghi^{23b}, J. Albert¹⁶⁴, P. Albicocco⁵³, S. Alderweireldt⁵², M. Aleksa³⁶,
I.N. Aleksandrov³⁸, C. Alexa^{27b}, T. Alexopoulos¹⁰, A. Alfonsi¹¹³, F. Alfonsi^{23b}, M. Alhroob¹¹⁹,
B. Ali¹³¹, S. Ali¹⁴⁷, M. Aliev³⁷, G. Alimonti^{70a}, W. Alkahi⁵⁵, C. Allaire⁶⁶, B.M.M. Allbrooke¹⁴⁵,
P.P. Allport²⁰, A. Aloisio^{71a,71b}, F. Alonso⁸⁹, C. Alpigiani¹³⁷, E. Alunno Camelia^{75a,75b},
M. Alvarez Estevez⁹⁸, M.G. Alviggi^{71a,71b}, M. Aly¹⁰⁰, Y. Amaral Coutinho^{81b}, A. Ambler¹⁰³,
C. Amelung³⁶, M. Amerl¹, C.G. Ames¹⁰⁸, D. Amidei¹⁰⁵, S.P. Amor Dos Santos^{129a},
S. Amoroso⁴⁸, K.R. Amos¹⁶², V. Ananiev¹²⁴, C. Anastopoulos¹³⁸, T. Andeen¹¹, J.K. Anders¹⁹,
S.Y. Andrean^{47a,47b}, A. Andreatta^{70a,70b}, S. Angelidakis⁹, A. Angerami^{41,ad}, A.V. Anisenkov³⁷,
A. Annovi^{73a}, C. Antel⁵⁶, M.T. Anthony¹³⁸, E. Antipov¹²⁰, M. Antonelli⁵³, D.J.A. Antrim^{17a},
F. Anulli^{74a}, M. Aoki⁸², T. Aoki¹⁵², J.A. Aparisi Pozo¹⁶², M.A. Aparo¹⁴⁵, L. Aperio Bella⁴⁸,
C. Appelt¹⁸, N. Aranzabal³⁶, V. Araujo Ferraz^{81a}, C. Arcangeletti⁵³, A.T.H. Arce⁵¹, E. Arena⁹¹,
J-F. Arguin¹⁰⁷, S. Argyropoulos⁵⁴, J.-H. Arling⁴⁸, A.J. Armbruster³⁶, O. Arnaez¹⁵⁴, H. Arnold¹¹³,
Z.P. Arrubarrena Tame¹⁰⁸, G. Artoni^{74a,74b}, H. Asada¹¹⁰, K. Asai¹¹⁷, S. Asai¹⁵², N.A. Asbah⁶¹,
J. Assahsah^{35d}, K. Assamagan²⁹, R. Astalos^{28a}, R.J. Atkin^{33a}, M. Atkinson¹⁶¹, N.B. Atlay¹⁸,
H. Atmani^{62b}, P.A. Atlasiddha¹⁰⁵, K. Augsten¹³¹, S. Auricchio^{71a,71b}, A.D. Auriol²⁰,
V.A. Austrup¹⁷⁰, G. Avner¹⁴⁹, G. Avolio³⁶, K. Axiotis⁵⁶, M.K. Ayoub^{14c}, G. Azuelos^{107,ai},
D. Babal^{28a}, H. Bachacou¹³⁴, K. Bachas^{151,s}, A. Bachi³⁴, F. Backman^{47a,47b}, A. Badea⁶¹,
P. Bagnaia^{74a,74b}, M. Bahmani¹⁸, A.J. Bailey¹⁶², V.R. Bailey¹⁶¹, J.T. Baines¹³³, C. Bakalis¹⁰,
O.K. Baker¹⁷¹, P.J. Bakker¹¹³, E. Bakos¹⁵, D. Bakshi Gupta⁸, S. Balaji¹⁴⁶,
R. Balasubramanian¹¹³, E.M. Baldin³⁷, P. Balek¹³², E. Ballabene^{70a,70b}, F. Balli¹³⁴,
L.M. Baltes^{63a}, W.K. Balunas³², J. Balz⁹⁹, E. Banas⁸⁵, M. Bandieramonte¹²⁸,
A. Bandyopadhyay²⁴, S. Bansal²⁴, L. Barak¹⁵⁰, E.L. Barberio¹⁰⁴, D. Barberis^{57b,57a},
M. Barbero¹⁰¹, G. Barbour⁹⁵, K.N. Barends^{33a}, T. Barillari¹⁰⁹, M-S. Barisits³⁶, T. Barklow¹⁴²,
R.M. Barnett^{17a}, P. Baron¹²¹, D.A. Baron Moreno¹⁰⁰, A. Baroncelli^{62a}, G. Barone²⁹, A.J. Barr¹²⁵,
L. Barranco Navarro^{47a,47b}, F. Barreiro⁹⁸, J. Barreiro Guimarães da Costa^{14a}, U. Barron¹⁵⁰,
M.G. Barros Teixeira^{129a}, S. Barsov³⁷, F. Bartels^{63a}, R. Bartoldus¹⁴², A.E. Barton⁹⁰, P. Bartos^{28a},
A. Basalae⁴⁸, A. Basan⁹⁹, M. Baselga⁴⁹, I. Bashta^{76a,76b}, A. Bassalat^{66,b}, M.J. Basso¹⁵⁴,
C.R. Basson¹⁰⁰, R.L. Bates⁵⁹, S. Batlamous^{35e}, J.R. Batley³², B. Batool¹⁴⁰, M. Battaglia¹³⁵,
D. Battulga¹⁸, M. Bauce^{74a,74b}, P. Bauer²⁴, A. Bayirli^{21a}, J.B. Beacham⁵¹, T. Beau¹²⁶,
P.H. Beauchemin¹⁵⁷, F. Becherer⁵⁴, P. Bechtel²⁴, H.P. Beck^{19,r}, K. Becker¹⁶⁶, A.J. Beddall^{21d},
V.A. Bednyakov³⁸, C.P. Bee¹⁴⁴, L.J. Beemster¹⁵, T.A. Beermann³⁶, M. Begalli^{81d}, M. Begel²⁹,
A. Behera¹⁴⁴, J.K. Behr⁴⁸, C. Beirao Da Cruz E Silva³⁶, J.F. Beirer^{55,36}, F. Beisiegel²⁴,
M. Belfkir¹⁵⁸, G. Bella¹⁵⁰, L. Bellagamba^{23b}, A. Bellerive³⁴, P. Bellos²⁰, K. Beloborodov³⁷,
K. Belotskiy³⁷, N.L. Belyaev³⁷, D. Benckekroun^{35a}, F. Bendebba^{35a}, Y. Benhammou¹⁵⁰,

D.P. Benjamin²⁹, M. Benoit²⁹, J.R. Bensinger²⁶, S. Bentvelsen¹¹³, L. Beresford³⁶, M. Beretta⁵³,
 D. Berge¹⁸, E. Bergeaas Kuutmann¹⁶⁰, N. Berger⁴, B. Bergmann¹³¹, J. Beringer^{17a}, S. Berlendis⁷,
 G. Bernardi⁵, C. Bernius¹⁴², F.U. Bernlochner²⁴, T. Berry⁹⁴, P. Berta¹³², A. Berthold⁵⁰,
 I.A. Bertram⁹⁰, S. Bethke¹⁰⁹, A. Betti^{74a,74b}, A.J. Bevan⁹³, M. Bhamjee^{33c}, S. Bhatta¹⁴⁴,
 D.S. Bhattacharya¹⁶⁵, P. Bhattarai²⁶, V.S. Bhopatkar¹²⁰, R. Bi^{29,al}, R.M. Bianchi¹²⁸, O. Biebel¹⁰⁸,
 R. Bielski¹²², M. Biglietti^{76a}, T.R.V. Billoud¹³¹, M. Bindi⁵⁵, A. Bingul^{21b}, C. Bini^{74a,74b},
 S. Biondi^{23b,23a}, A. Biondini⁹¹, C.J. Birch-sykes¹⁰⁰, G.A. Bird^{20,133}, M. Birman¹⁶⁸, T. Bisanz³⁶,
 E. Bisceglie^{43b,43a}, D. Biswas^{169,1}, A. Bitadze¹⁰⁰, K. Bjørke¹²⁴, I. Bloch⁴⁸, C. Blocker²⁶,
 A. Blue⁵⁹, U. Blumenschein⁹³, J. Blumenthal⁹⁹, G.J. Bobbink¹¹³, V.S. Bobrovnikov³⁷,
 M. Boehler⁵⁴, D. Bogovac³⁶, A.G. Bogdanchikov³⁷, C. Bohm^{47a}, V. Boisvert⁹⁴, P. Bokan⁴⁸,
 T. Bold^{84a}, M. Bomben⁵, M. Bona⁹³, M. Boonekamp¹³⁴, C.D. Booth⁹⁴, A.G. Borbély⁵⁹,
 H.M. Borecka-Bielska¹⁰⁷, L.S. Borgna⁹⁵, G. Borissov⁹⁰, D. Bortoletto¹²⁵, D. Boscherini^{23b},
 M. Bosman¹³, J.D. Bossio Sola³⁶, K. Bouaouda^{35a}, N. Bouchhar¹⁶², J. Boudreau¹²⁸,
 E.V. Bouhova-Thacker⁹⁰, D. Boumediene⁴⁰, R. Bouquet⁵, A. Boveia¹¹⁸, J. Boyd³⁶, D. Boye²⁹,
 I.R. Boyko³⁸, J. Bracinik²⁰, N. Brahimi^{62d}, G. Brandt¹⁷⁰, O. Brandt³², F. Braren⁴⁸, B. Brau¹⁰²,
 J.E. Brau¹²², K. Brendlinger⁴⁸, R. Brenner¹⁶⁸, L. Brenner¹¹³, R. Brenner¹⁶⁰, S. Bressler¹⁶⁸,
 B. Brickwedde⁹⁹, D. Britton⁵⁹, D. Britzger¹⁰⁹, I. Brock²⁴, G. Brooijmans⁴¹, W.K. Brooks^{136f},
 E. Brost²⁹, T.L. Bruckler¹²⁵, P.A. Bruckman de Renstrom⁸⁵, B. Brüers⁴⁸, D. Bruncko^{28b,*},
 A. Bruni^{23b}, G. Bruni^{23b}, M. Bruschi^{23b}, N. Bruscano^{74a,74b}, L. Bryngemark¹⁴², T. Buanes¹⁶,
 Q. Buat¹³⁷, P. Buchholz¹⁴⁰, A.G. Buckley⁵⁹, I.A. Budagov^{38,*}, M.K. Bugge¹²⁴, O. Bulekov³⁷,
 B.A. Bullard⁶¹, S. Burdin⁹¹, C.D. Burgard⁴⁸, A.M. Burger⁴⁰, B. Burghgrave⁸, J.T.P. Burr³²,
 C.D. Burton¹¹, J.C. Burzynski¹⁴¹, E.L. Busch⁴¹, V. Büscher⁹⁹, P.J. Bussey⁵⁹, J.M. Butler²⁵,
 C.M. Buttar⁵⁹, J.M. Butterworth⁹⁵, W. Buttinger¹³³, C.J. Buxo Vazquez¹⁰⁶, A.R. Buzykaev³⁷,
 G. Cabras^{23b}, S. Cabrera Urbán¹⁶², D. Caforio⁵⁸, H. Cai¹²⁸, Y. Cai^{14a,14d}, V.M.M. Cairo³⁶,
 O. Cakir^{3a}, N. Calace³⁶, P. Calafiura^{17a}, G. Calderini¹²⁶, P. Calfayan⁶⁷, G. Callea⁵⁹,
 L.P. Caloba^{81b}, D. Calvet⁴⁰, S. Calvet⁴⁰, T.P. Calvet¹⁰¹, M. Calvetti^{73a,73b}, R. Camacho Toro¹²⁶,
 S. Camarda³⁶, D. Camarero Munoz²⁶, P. Camarri^{75a,75b}, M.T. Camerlingo^{76a,76b}, D. Cameron¹²⁴,
 C. Camincher¹⁶⁴, M. Campanelli⁹⁵, A. Camplani⁴², V. Canale^{71a,71b}, A. Canesse¹⁰³,
 M. Cano Bret⁷⁹, J. Cantero¹⁶², Y. Cao¹⁶¹, F. Capocasa²⁶, M. Capua^{43b,43a}, A. Carbone^{70a,70b},
 R. Cardarelli^{75a}, J.C.J. Cardenas⁸, F. Cardillo¹⁶², T. Carli³⁶, G. Carlino^{71a}, J.I. Carlotto¹³,
 B.T. Carlson^{128,t}, E.M. Carlson^{164,155a}, L. Carminati^{70a,70b}, M. Carnesale^{74a,74b}, S. Caron¹¹²,
 E. Carquin^{136f}, S. Carrá^{70a,70b}, G. Carratta^{23b,23a}, F. Carrio Argos^{33g}, J.W.S. Carter¹⁵⁴,
 T.M. Carter⁵², M.P. Casado^{13,i}, A.F. Casha¹⁵⁴, E.G. Castiglia¹⁷¹, F.L. Castillo^{63a},
 L. Castillo Garcia¹³, V. Castillo Gimenez¹⁶², N.F. Castro^{129a,129e}, A. Catinaccio³⁶,
 J.R. Catmore¹²⁴, V. Cavaliere²⁹, N. Cavalli^{23b,23a}, V. Cavalinni^{73a,73b}, E. Celebi^{21a}, F. Celli¹²⁵,
 M.S. Centonze^{69a,69b}, K. Cerny¹²¹, A.S. Cerqueira^{81a}, A. Cerri¹⁴⁵, L. Cerrito^{75a,75b}, F. Cerutti^{17a},
 A. Cervelli^{23b}, S.A. Cetin^{21d}, Z. Chadi^{35a}, D. Chakraborty¹¹⁴, M. Chala^{129f}, J. Chan¹⁶⁹,
 W.Y. Chan¹⁵², J.D. Chapman³², B. Chargeishvili^{148b}, D.G. Charlton²⁰, T.P. Charman⁹³,
 M. Chatterjee¹⁹, S. Chekanov⁶, S.V. Chekulaev^{155a}, G.A. Chelkov^{38,a}, A. Chen¹⁰⁵, B. Chen¹⁵⁰,
 B. Chen¹⁶⁴, C. Chen^{62a}, H. Chen^{14c}, H. Chen²⁹, J. Chen^{62c}, J. Chen²⁶, S. Chen¹⁵², S.J. Chen^{14c},
 X. Chen^{62c}, X. Chen^{14b,ah}, Y. Chen^{62a}, C.L. Cheng¹⁶⁹, H.C. Cheng^{64a}, S. Cheong¹⁴²,
 A. Cheplakov³⁸, E. Cheremushkina⁴⁸, E. Cherepanova¹¹³, R. Cherkaoui El Moursli^{35e}, E. Cheu⁷,
 K. Cheung⁶⁵, L. Chevalier¹³⁴, V. Chiarella⁵³, G. Chiarelli^{73a}, N. Chiedde¹⁰¹, G. Chiodini^{69a},

A.S. Chisholm²⁰, A. Chitan^{27b}, M. Chitishvili¹⁶², Y.H. Chiu¹⁶⁴, M.V. Chizhov³⁸, K. Choi¹¹,
 A.R. Chomont^{74a,74b}, Y. Chou¹⁰², E.Y.S. Chow¹¹³, T. Chowdhury^{33g}, L.D. Christopher^{33g},
 K.L. Chu^{64a}, M.C. Chu^{64a}, X. Chu^{14a,14d}, J. Chudoba¹³⁰, J.J. Chwastowski⁸⁵, D. Cieri¹⁰⁹,
 K.M. Ciesla^{84a}, V. Cindro⁹², A. Ciocio^{17a}, F. Ciroto^{71a,71b}, Z.H. Citron^{168,m}, M. Citterio^{70a},
 D.A. Ciubotaru^{27b}, B.M. Ciungu¹⁵⁴, A. Clark⁵⁶, P.J. Clark⁵², J.M. Clavijo Columbie⁴⁸,
 S.E. Clawson¹⁰⁰, C. Clement^{47a,47b}, J. Clercx⁴⁸, L. Clissa^{23b,23a}, Y. Coadou¹⁰¹, M. Cobal^{168a,68c},
 A. Coccaro^{57b}, R.F. Coelho Barrue^{129a}, R. Coelho Lopes De Sa¹⁰², S. Coelli^{70a}, H. Cohen¹⁵⁰,
 A.E.C. Coimbra^{70a,70b}, B. Cole⁴¹, J. Collot⁶⁰, P. Conde Muiño^{129a,129g}, M.P. Connell^{33c},
 S.H. Connell^{33c}, I.A. Connelly⁵⁹, E.I. Conroy¹²⁵, F. Conventi^{71a,aj}, H.G. Cooke²⁰,
 A.M. Cooper-Sarkar¹²⁵, F. Cormier¹⁶³, L.D. Corpe³⁶, M. Corradi^{74a,74b}, E.E. Corrigan⁹⁷,
 F. Corriveau^{103,y}, A. Cortes-Gonzalez¹⁸, M.J. Costa¹⁶², F. Costanza⁴, D. Costanzo¹³⁸,
 B.M. Cote¹¹⁸, G. Cowan⁹⁴, J.W. Cowley³², K. Cranmer¹¹⁶, S. Crépe-Renaudin⁶⁰, F. Crescioli¹²⁶,
 M. Cristinziani¹⁴⁰, M. Cristoforetti^{77a,77b,d}, V. Croft¹⁵⁷, G. Crosetti^{43b,43a}, A. Cueto³⁶,
 T. Cuhadar Donszelmann¹⁵⁹, H. Cui^{14a,14d}, Z. Cui⁷, A.R. Cukierman¹⁴², W.R. Cunningham⁵⁹,
 F. Curcio^{43b,43a}, P. Czodrowski³⁶, M.M. Czurylo^{63b}, M.J. Da Cunha Sargedas De Sousa^{62a},
 J.V. Da Fonseca Pinto^{81b}, C. Da Via¹⁰⁰, W. Dabrowski^{84a}, T. Dado⁴⁹, S. Dahbi^{33g}, T. Dai¹⁰⁵,
 C. Dallapiccola¹⁰², M. Dam⁴², G. D'amen²⁹, V. D'Amico¹⁰⁸, J. Damp⁹⁹, J.R. Dandoy¹²⁷,
 M.F. Daneri³⁰, M. Danninger¹⁴¹, V. Dao³⁶, G. Darbo^{57b}, S. Darmora⁶, S.J. Das^{29,al},
 S. D'Auria^{70a,70b}, C. David^{155b}, T. Davidek¹³², D.R. Davis⁵¹, B. Davis-Purcell³⁴, I. Dawson⁹³,
 K. De⁸, R. De Asmundis^{71a}, M. De Beurs¹¹³, N. De Biase⁴⁸, S. De Castro^{23b,23a}, N. De Groot¹¹²,
 P. de Jong¹¹³, H. De la Torre¹⁰⁶, A. De Maria^{14c}, A. De Salvo^{74a}, U. De Sanctis^{75a,75b},
 A. De Santo¹⁴⁵, J.B. De Vivie De Regie⁶⁰, D.V. Dedovich³⁸, J. Degens¹¹³, A.M. Deiana⁴⁴,
 F. Del Corso^{23b,23a}, J. Del Peso⁹⁸, F. Del Rio^{63a}, F. Deliot¹³⁴, C.M. Delitzsch⁴⁹,
 M. Della Pietra^{71a,71b}, D. Della Volpe⁵⁶, A. Dell'Acqua³⁶, L. Dell'Asta^{70a,70b}, M. Delmastro⁴,
 P.A. Delsart⁶⁰, S. Demers¹⁷¹, M. Demichev³⁸, S.P. Denisov³⁷, L. D'Eramo¹¹⁴, D. Derendarz⁸⁵,
 F. Derue¹²⁶, P. Dervan⁹¹, K. Desch²⁴, K. Dette¹⁵⁴, C. Deutsch²⁴, P.O. Deviveiros³⁶,
 F.A. Di Bello^{74a,74b}, A. Di Ciaccio^{75a,75b}, L. Di Ciaccio⁴, A. Di Domenico^{74a,74b},
 C. Di Donato^{71a,71b}, A. Di Girolamo³⁶, G. Di Gregorio^{73a,73b}, A. Di Luca^{77a,77b},
 B. Di Micco^{76a,76b}, R. Di Nardo^{76a,76b}, C. Diaconu¹⁰¹, F.A. Dias¹¹³, T. Dias Do Vale¹⁴¹,
 M.A. Diaz^{136a,136b}, F.G. Diaz Capriles²⁴, M. Didenko¹⁶², E.B. Diehl¹⁰⁵, L. Diehl⁵⁴,
 S. Díez Cornell⁴⁸, C. Diez Pardos¹⁴⁰, C. Dimitriadi^{24,160}, A. Dimitrievska^{17a}, W. Ding^{14b},
 J. Dingfelder²⁴, I-M. Dinu^{27b}, S.J. Dittmeier^{63b}, F. Dittus³⁶, F. Djama¹⁰¹, T. Djobava^{148b},
 J.I. Djuvsland¹⁶, C. Doglioni^{100,97}, J. Dolejsi¹³², Z. Dolezal¹³², M. Donadelli^{81c}, B. Dong^{62c},
 J. Donini⁴⁰, A. D'Onofrio^{14c}, M. D'Onofrio⁹¹, J. Dopke¹³³, A. Doria^{71a}, M.T. Dova⁸⁹,
 A.T. Doyle⁵⁹, M.A. Dragnet¹²⁵, E. Drechsler¹⁴¹, E. Dreyer¹⁶⁸, I. Drivas-koulouris¹⁰,
 A.S. Drobac¹⁵⁷, M. Drozdova⁵⁶, D. Du^{62a}, T.A. du Pree¹¹³, F. Dubinin³⁷, M. Dubovsky^{28a},
 E. Duchovni¹⁶⁸, G. Duckeck¹⁰⁸, O.A. Ducu^{27b}, D. Duda¹⁰⁹, A. Dudarev³⁶, M. D'uffizi¹⁰⁰,
 L. Duflot⁶⁶, M. Dührssen³⁶, C. Dülsen¹⁷⁰, A.E. Dumitriu^{27b}, M. Dunford^{63a}, S. Dungs⁴⁹,
 K. Dunne^{47a,47b}, A. Duperrin¹⁰¹, H. Duran Yildiz^{3a}, M. Düren⁵⁸, A. Durglishvili^{148b},
 B.L. Dwyer¹¹⁴, G.I. Dyckes^{17a}, M. Dyndal^{84a}, S. Dysch¹⁰⁰, B.S. Dziedzic⁸⁵, Z.O. Earnshaw¹⁴⁵,
 B. Eckerova^{28a}, M.G. Eggleston⁵¹, E. Egidio Purcino De Souza^{81b}, L.F. Ehrke⁵⁶, G. Eigen¹⁶,
 K. Einsweiler^{17a}, T. Ekelof¹⁶⁰, P.A. Ekman⁹⁷, Y. El Ghazali^{35b}, H. El Jarrari^{35e,147},
 A. El Moussaouy^{35a}, V. Ellajosyula¹⁶⁰, M. Ellert¹⁶⁰, F. Ellinghaus¹⁷⁰, A.A. Elliot⁹³, N. Ellis³⁶,

J. Elmsheuser²⁹, M. Elsing³⁶, D. Emeliyanov¹³³, A. Emerman⁴¹, Y. Enari¹⁵², I. Ene^{17a}, S. Epari¹³, J. Erdmann^{49,af}, A. Ereditato¹⁹, P.A. Erland⁸⁵, M. Errenst¹⁷⁰, M. Escalier⁶⁶, C. Escobar¹⁶², E. Etzion¹⁵⁰, G. Evans^{129a}, H. Evans⁶⁷, M.O. Evans¹⁴⁵, A. Ezhilov³⁷, S. Ezzarqtouni^{35a}, F. Fabbri⁵⁹, L. Fabbri^{23b,23a}, G. Facini⁹⁵, V. Fadeyev¹³⁵, R.M. Fakhrutdinov³⁷, S. Falciano^{74a}, P.J. Falke²⁴, S. Falke³⁶, J. Faltova¹³², Y. Fan^{14a}, Y. Fang^{14a,14d}, G. Fanourakis⁴⁶, M. Fanti^{70a,70b}, M. Faraj^{68a,68b}, A. Farbin⁸, A. Farilla^{76a}, T. Farooque¹⁰⁶, S.M. Farrington⁵², F. Fassi^{35e}, D. Fassouliotis⁹, M. Fauci Giannelli^{75a,75b}, W.J. Fawcett³², L. Fayard⁶⁶, P. Federicova¹³⁰, O.L. Fedin^{37,a}, G. Fedotov³⁷, M. Feickert¹⁶¹, L. Feligioni¹⁰¹, A. Fell¹³⁸, D.E. Fellers¹²², C. Feng^{62b}, M. Feng^{14b}, Z. Feng¹¹³, M.J. Fenton¹⁵⁹, A.B. Fenyuk³⁷, L. Ferencz⁴⁸, S.W. Ferguson⁴⁵, J. Ferrando⁴⁸, A. Ferrari¹⁶⁰, P. Ferrari^{113,112}, R. Ferrari^{72a}, D. Ferrere⁵⁶, C. Ferretti¹⁰⁵, F. Fiedler⁹⁹, A. Filipčić⁹², E.K. Filmer¹, F. Filthaut¹¹², M.C.N. Fiolhais^{129a,129c,c}, L. Fiorini¹⁶², F. Fischer¹⁴⁰, W.C. Fisher¹⁰⁶, T. Fitschen²⁰, I. Fleck¹⁴⁰, P. Fleischmann¹⁰⁵, T. Flick¹⁷⁰, L. Flores¹²⁷, M. Flores^{33d,ae}, L.R. Flores Castillo^{64a}, F.M. Follega^{77a,77b}, N. Fomin¹⁶, J.H. Foo¹⁵⁴, B.C. Forland⁶⁷, A. Formica¹³⁴, A.C. Forti¹⁰⁰, E. Fortin¹⁰¹, A.W. Fortman⁶¹, M.G. Foti^{17a}, L. Fountas^{9j}, D. Fournier⁶⁶, H. Fox⁹⁰, P. Francavilla^{73a,73b}, S. Francescato⁶¹, M. Franchini^{23b,23a}, S. Franchino^{63a}, D. Francis³⁶, L. Franco¹¹², L. Franconi¹⁹, M. Franklin⁶¹, G. Frattari²⁶, A.C. Freegard⁹³, P.M. Freeman²⁰, W.S. Freund^{81b}, N. Fritzsche⁵⁰, A. Froch⁵⁴, D. Froidevaux³⁶, J.A. Frost¹²⁵, Y. Fu^{62a}, M. Fujimoto¹¹⁷, E. Fullana Torregrosa^{162,*}, J. Fuster¹⁶², A. Gabrielli^{23b,23a}, A. Gabrielli¹⁵⁴, P. Gadov⁴⁸, G. Gagliardi^{57b,57a}, L.G. Gagnon^{17a}, G.E. Gallardo¹²⁵, E.J. Gallas¹²⁵, B.J. Gallop¹³³, R. Gamboa Goni⁹³, K.K. Gan¹¹⁸, S. Ganguly¹⁵², J. Gao^{62a}, Y. Gao⁵², F.M. Garay Walls^{136a,136b}, B. Garcia^{29,al}, C. García¹⁶², J.E. García Navarro¹⁶², J.A. García Pascual^{14a}, M. Garcia-Sciveres^{17a}, R.W. Gardner³⁹, D. Garg⁷⁹, R.B. Garg^{142,q}, S. Gargiulo⁵⁴, C.A. Garner¹⁵⁴, V. Garonne²⁹, S.J. Gasiorowski¹³⁷, P. Gaspar^{81b}, G. Gaudio^{72a}, V. Gautam¹³, P. Gauzzi^{74a,74b}, I.L. Gavrilenko³⁷, A. Gavriluk³⁷, C. Gay¹⁶³, G. Gaycken⁴⁸, E.N. Gazis¹⁰, A.A. Geanta^{27b,27e}, C.M. Gee¹³⁵, J. Geisen⁹⁷, M. Geisen⁹⁹, C. Gemme^{57b}, M.H. Genest⁶⁰, S. Gentile^{74a,74b}, S. George⁹⁴, W.F. George²⁰, T. Gerialis⁴⁶, L.O. Gerlach⁵⁵, P. Gessinger-Befurt³⁶, M. Ghasemi Bostanabad¹⁶⁴, M. Ghneimat¹⁴⁰, K. Ghorbanian⁹³, A. Ghosal¹⁴⁰, A. Ghosh¹⁵⁹, A. Ghosh⁷, B. Giacobbe^{23b}, S. Giagu^{74a,74b}, N. Giangiacomi¹⁵⁴, P. Giannetti^{73a}, A. Giannini^{62a}, S.M. Gibson⁹⁴, M. Gignac¹³⁵, D.T. Gil^{84b}, A.K. Gilbert^{84a}, B.J. Gilbert⁴¹, D. Gillberg³⁴, G. Gilles¹¹³, N.E.K. Gillwald⁴⁸, L. Ginabat¹²⁶, D.M. Gingrich^{2,ai}, M.P. Giordani^{68a,68c}, P.F. Giraud¹³⁴, G. Giugliarelli^{68a,68c}, D. Giugni^{70a}, F. Giuli³⁶, I. Gkialas^{9j}, L.K. Gladilin³⁷, C. Glasman⁹⁸, G.R. Gledhill¹²², M. Glisic¹²², I. Gnesi^{43b,f}, Y. Go^{29,al}, M. Goblirsch-Kolb²⁶, B. Gocke⁴⁹, D. Godin¹⁰⁷, S. Goldfarb¹⁰⁴, T. Golling⁵⁶, M.G.D. Gololo^{33g}, D. Golubkov³⁷, J.P. Gombas¹⁰⁶, A. Gomes^{129a,129b}, G. Gomes Da Silva¹⁴⁰, A.J. Gomez Delegido¹⁶², R. Goncalves Gama⁵⁵, R. Gonçalves^{129a,129c}, G. Gonella¹²², L. Gonella²⁰, A. Gongadze³⁸, F. Gonnella²⁰, J.L. Gonski⁴¹, R.Y. González Andana⁵², S. González de la Hoz¹⁶², S. Gonzalez Fernandez¹³, R. Gonzalez Lopez⁹¹, C. Gonzalez Renteria^{17a}, R. Gonzalez Suarez¹⁶⁰, S. Gonzalez-Sevilla⁵⁶, G.R. Gonzalvo Rodriguez¹⁶², L. Goossens³⁶, N.A. Gorasia²⁰, P.A. Gorbounov³⁷, B. Gorini³⁶, E. Gorini^{69a,69b}, A. Gorišek⁹², A.T. Goshaw⁵¹, M.I. Gostkin³⁸, C.A. Gottardo³⁶, M. Gouighri^{35b}, V. Goumarre⁴⁸, A.G. Goussiou¹³⁷, N. Govender^{33c}, C. Goy⁴, I. Grabowska-Bold^{84a}, K. Graham³⁴, E. Gramstad¹²⁴, S. Grancagnolo¹⁸, M. Grandi¹⁴⁵, V. Gratchev^{37,*}, P.M. Gravila^{27f}, F.G. Gravili^{69a,69b}, H.M. Gray^{17a}, M. Greco^{69a,69b}, C. Grefe²⁴, I.M. Gregor⁴⁸, P. Grenier¹⁴²,

C. Grieco¹³, A.A. Grillo¹³⁵, K. Grimm^{31,n}, S. Grinstein^{13,v}, J.-F. Grivaz⁶⁶, E. Gross¹⁶⁸,
 J. Grosse-Knetter⁵⁵, C. Grud¹⁰⁵, A. Grummer¹¹¹, J.C. Grundy¹²⁵, L. Guan¹⁰⁵, W. Guan¹⁶⁹,
 C. Gubbels¹⁶³, J.G.R. Guerrero Rojas¹⁶², G. Guerrieri^{68a,68b}, F. Guescini¹⁰⁹, R. Gugel⁹⁹,
 J.A.M. Guhit¹⁰⁵, A. Guida⁴⁸, T. Guillemain⁴, E. Guilloton^{166,133}, S. Guindon³⁶, F. Guo^{14a,14d},
 J. Guo^{62c}, L. Guo⁶⁶, Y. Guo¹⁰⁵, R. Gupta⁴⁸, S. Gurbuz²⁴, S.S. Gurdasani⁵⁴, G. Gustavino³⁶,
 M. Guth⁵⁶, P. Gutierrez¹¹⁹, L.F. Gutierrez Zagazeta¹²⁷, C. Gutschow⁹⁵, C. Guyot¹³⁴,
 C. Gwenlan¹²⁵, C.B. Gwilliam⁹¹, E.S. Haaland¹²⁴, A. Haas¹¹⁶, M. Habedank⁴⁸, C. Haber^{17a},
 H.K. Hadavand⁸, A. Hadeif⁹⁹, S. Hadzic¹⁰⁹, E.H. Haines⁹⁵, M. Haleem¹⁶⁵, J. Haley¹²⁰,
 J.J. Hall¹³⁸, G.D. Hallelwell¹⁰¹, L. Halser¹⁹, K. Hamano¹⁶⁴, H. Hamdaoui^{35e}, M. Hamer²⁴,
 G.N. Hamity⁵², J. Han^{62b}, K. Han^{62a}, L. Han^{14c}, L. Han^{62a}, S. Han^{17a}, Y.F. Han¹⁵⁴,
 K. Hanagaki⁸², M. Hance¹³⁵, D.A. Hangal^{41,ad}, H. Hanif¹⁴¹, M.D. Hank³⁹, R. Hankache¹⁰⁰,
 J.B. Hansen⁴², J.D. Hansen⁴², P.H. Hansen⁴², K. Hara¹⁵⁶, D. Harada⁵⁶, T. Harenberg¹⁷⁰,
 S. Harkusha³⁷, Y.T. Harris¹²⁵, N.M. Harrison¹¹⁸, P.F. Harrison¹⁶⁶, N.M. Hartman¹⁴²,
 N.M. Hartmann¹⁰⁸, Y. Hasegawa¹³⁹, A. Hasib⁵², S. Haug¹⁹, R. Hauser¹⁰⁶, M. Havranek¹³¹,
 C.M. Hawkes²⁰, R.J. Hawkins³⁶, S. Hayashida¹¹⁰, D. Hayden¹⁰⁶, C. Hayes¹⁰⁵, R.L. Hayes¹⁶³,
 C.P. Hays¹²⁵, J.M. Hays⁹³, H.S. Hayward⁹¹, F. He^{62a}, Y. He¹⁵³, Y. He¹²⁶, M.P. Heath⁵²,
 V. Hedberg⁹⁷, A.L. Heggelund¹²⁴, N.D. Hehir⁹³, C. Heidegger⁵⁴, K.K. Heidegger⁵⁴,
 W.D. Heidorn⁸⁰, J. Heilman³⁴, S. Heim⁴⁸, T. Heim^{17a}, J.G. Heinlein¹²⁷, J.J. Heinrich¹²²,
 L. Heinrich^{109,ag}, J. Hejbal¹³⁰, L. Helary⁴⁸, A. Held¹⁶⁹, S. Hellesund¹²⁴, C.M. Helling¹⁶³,
 S. Hellman^{47a,47b}, C. Helsen³⁶, R.C.W. Henderson⁹⁰, L. Henkelmann³²,
 A.M. Henriques Correia³⁶, H. Herde⁹⁷, Y. Hernández Jiménez¹⁴⁴, L.M. Herrmann²⁴,
 M.G. Herrmann¹⁰⁸, T. Herrmann⁵⁰, G. Hertzen⁵⁴, R. Hertzenberger¹⁰⁸, L. Hervas³⁶,
 N.P. Hessey^{155a}, H. Hibi⁸³, E. Higón-Rodríguez¹⁶², S.J. Hillier²⁰, I. Hinchliffe^{17a},
 F. Hinterkeuser²⁴, M. Hirose¹²³, S. Hirose¹⁵⁶, D. Hirschbuehl¹⁷⁰, T.G. Hitchings¹⁰⁰, B. Hiti⁹²,
 J. Hobbs¹⁴⁴, R. Hobincu^{27e}, N. Hod¹⁶⁸, M.C. Hodgkinson¹³⁸, B.H. Hodgkinson³², A. Hoecker³⁶,
 J. Hofer⁴⁸, D. Hohn⁵⁴, T. Holm²⁴, M. Holzbock¹⁰⁹, L.B.A.H. Hommels³², B.P. Honan¹⁰⁰,
 J. Hong^{62c}, T.M. Hong¹²⁸, Y. Hong⁵⁵, J.C. Honig⁵⁴, A. Hönle¹⁰⁹, B.H. Hooberman¹⁶¹,
 W.H. Hopkins⁶, Y. Horii¹¹⁰, S. Hou¹⁴⁷, A.S. Howard⁹², J. Howarth⁵⁹, J. Hoya⁶, M. Hrabovsky¹²¹,
 A. Hrynevich⁴⁸, T. Hryn'ova⁴, P.J. Hsu⁶⁵, S.-C. Hsu¹³⁷, Q. Hu^{41,ad}, Y.F. Hu^{14a,14d,ak},
 D.P. Huang⁹⁵, S. Huang^{64b}, X. Huang^{14c}, Y. Huang^{62a}, Y. Huang^{14a}, Z. Huang¹⁰⁰, Z. Hubacek¹³¹,
 M. Huebner²⁴, F. Huegging²⁴, T.B. Huffman¹²⁵, M. Huhtinen³⁶, S.K. Huiberts¹⁶, R. Hulsken¹⁰³,
 N. Huseynov^{12,a}, J. Huston¹⁰⁶, J. Huth⁶¹, R. Hyneman¹⁴², S. Hyrych^{28a}, G. Iacobucci⁵⁶,
 G. Iakovidis²⁹, I. Ibragimov¹⁴⁰, L. Iconomidou-Fayard⁶⁶, P. Iengo^{71a,71b}, R. Iguchi¹⁵²,
 T. Iizawa⁵⁶, Y. Ikegami⁸², A. Ilg¹⁹, N. Ilic¹⁵⁴, H. Imam^{35a}, T. Ingebretsen Carlson^{47a,47b},
 G. Introzzi^{72a,72b}, M. Iodice^{76a}, V. Ippolito^{74a,74b}, M. Ishino¹⁵², W. Islam¹⁶⁹, C. Issever^{18,48},
 S. Istin^{21a,an}, H. Ito¹⁶⁷, J.M. Iturbe Ponce^{64a}, R. Iuppa^{77a,77b}, A. Ivina¹⁶⁸, J.M. Izen⁴⁵, V. Izzo^{71a},
 P. Jacka^{130,131}, P. Jackson¹, R.M. Jacobs⁴⁸, B.P. Jaeger¹⁴¹, C.S. Jagfeld¹⁰⁸, G. Jäkel¹⁷⁰,
 K. Jakobs⁵⁴, T. Jakoubek¹⁶⁸, J. Jamieson⁵⁹, K.W. Janas^{84a}, G. Jarlskog⁹⁷, A.E. Jaspan⁹¹,
 M. Javurkova¹⁰², F. Jeanneau¹³⁴, L. Jeanty¹²², J. Jejelava^{148a,ab}, P. Jenni^{54,g}, C.E. Jessiman³⁴,
 S. Jézéquel⁴, J. Jia¹⁴⁴, X. Jia⁶¹, X. Jia^{14a,14d}, Z. Jia^{14c}, Y. Jiang^{62a}, S. Jiggins⁵²,
 J. Jimenez Pena¹⁰⁹, S. Jin^{14c}, A. Jinaru^{27b}, O. Jinnouchi¹⁵³, P. Johansson¹³⁸, K.A. Johns⁷,
 D.M. Jones³², E. Jones¹⁶⁶, P. Jones³², R.W.L. Jones⁹⁰, T.J. Jones⁹¹, R. Joshi¹¹⁸, J. Jovicevic¹⁵,
 X. Ju^{17a}, J.J. Junggeburth³⁶, A. Juste Rozas^{13,v}, S. Kabana^{136e}, A. Kaczmarska⁸⁵, M. Kado^{74a,74b},

H. Kagan¹¹⁸, M. Kagan¹⁴², A. Kahn⁴¹, A. Kahn¹²⁷, C. Kahra⁹⁹, T. Kaji¹⁶⁷, E. Kajomovitz¹⁴⁹,
 N. Kakati¹⁶⁸, C.W. Kalderon²⁹, A. Kamenshchikov¹⁵⁴, S. Kanayama¹⁵³, N.J. Kang¹³⁵,
 Y. Kano¹¹⁰, D. Kar^{33g}, K. Karava¹²⁵, M.J. Kareem^{155b}, E. Karentzos⁵⁴, I. Karkanias¹⁵¹,
 S.N. Karpov³⁸, Z.M. Karpova³⁸, V. Kartvelishvili⁹⁰, A.N. Karyukhin³⁷, E. Kasimi¹⁵¹, C. Kato^{62d},
 J. Katzy⁴⁸, S. Kaur³⁴, K. Kawade¹³⁹, K. Kawagoe⁸⁸, T. Kawamoto¹³⁴, G. Kawamura⁵⁵,
 E.F. Kay¹⁶⁴, F.I. Kaya¹⁵⁷, S. Kazakos¹³, V.F. Kazanin³⁷, Y. Ke¹⁴⁴, J.M. Keaveney^{33a},
 R. Keeler¹⁶⁴, G.V. Kehris⁶¹, J.S. Keller³⁴, A.S. Kelly⁹⁵, D. Kelsey¹⁴⁵, J.J. Kempster²⁰,
 K.E. Kennedy⁴¹, P.D. Kennedy⁹⁹, O. Kepka¹³⁰, B.P. Kerridge¹⁶⁶, S. Kersten¹⁷⁰, B.P. Kerševan⁹²,
 S. Keshri⁶⁶, L. Keszeghova^{28a}, S. Ketabchi Haghghat¹⁵⁴, M. Khandoga¹²⁶, A. Khanov¹²⁰,
 A.G. Kharlamov³⁷, T. Kharlamova³⁷, E.E. Khoda¹³⁷, T.J. Khoo¹⁸, G. Khoraiuli¹⁶⁵, J. Khubua^{148b},
 Y.A.R. Khwaira⁶⁶, M. Kiehn³⁶, A. Kilgallon¹²², D.W. Kim^{47a,47b}, E. Kim¹⁵³, Y.K. Kim³⁹,
 N. Kimura⁹⁵, A. Kirchhoff⁵⁵, D. Kirchmeier⁵⁰, C. Kirfel²⁴, J. Kirk¹³³, A.E. Kiryunin¹⁰⁹,
 T. Kishimoto¹⁵², D.P. Kisiuk¹⁵⁴, C. Kitsaki¹⁰, O. Kivernyk²⁴, M. Klassen^{63a}, C. Klein³⁴,
 L. Klein¹⁶⁵, M.H. Klein¹⁰⁵, M. Klein⁹¹, S.B. Klein⁵⁶, U. Klein⁹¹, P. Klimek³⁶, A. Klimentov²⁹,
 F. Klimpel¹⁰⁹, T. Klingl²⁴, T. Klioutchnikova³⁶, F.F. Klitzner¹⁰⁸, P. Kluit¹¹³, S. Kluth¹⁰⁹,
 E. Kneringer⁷⁸, T.M. Knight¹⁵⁴, A. Knue⁵⁴, D. Kobayashi⁸⁸, R. Kobayashi⁸⁶, M. Kocian¹⁴²,
 P. Kodyš¹³², D.M. Koeck¹⁴⁵, P.T. Koenig²⁴, T. Koffas³⁴, N.M. Köhler³⁶, M. Kolb¹³⁴, I. Koletsou⁴,
 T. Komarek¹²¹, K. Köneke⁵⁴, A.X.Y. Kong¹, T. Kono¹¹⁷, N. Konstantinidis⁹⁵, B. Konya⁹⁷,
 R. Kopeliansky⁶⁷, S. Koperny^{84a}, K. Korcyl⁸⁵, K. Kordas¹⁵¹, G. Koren¹⁵⁰, A. Korn⁹⁵, S. Korn⁵⁵,
 I. Korolkov¹³, N. Korotkova³⁷, B. Kortman¹¹³, O. Kortner¹⁰⁹, S. Kortner¹⁰⁹, W.H. Kostecka¹¹⁴,
 V.V. Kostyukhin¹⁴⁰, A. Kotsokechagia¹³⁴, A. Kotwal⁵¹, A. Koulouris³⁶,
 A. Kourkoumeli-Charalampidi^{72a,72b}, C. Kourkoumelis⁹, E. Kourlitis⁶, O. Kovanda¹⁴⁵,
 R. Kowalewski¹⁶⁴, W. Kozanecki¹³⁴, A.S. Kozhin³⁷, V.A. Kramarenko³⁷, G. Kramberger⁹²,
 P. Kramer⁹⁹, M.W. Krasny¹²⁶, A. Krasznahorkay³⁶, J.A. Kremer⁹⁹, T. Kresse⁵⁰, J. Kretzschmar⁹¹,
 K. Kreul¹⁸, P. Krieger¹⁵⁴, F. Krieter¹⁰⁸, S. Krishnamurthy¹⁰², A. Krishnan^{63b}, M. Krivos¹³²,
 K. Krizka^{17a}, K. Kroeninger⁴⁹, H. Kroha¹⁰⁹, J. Kroll¹³⁰, J. Kroll¹²⁷, K.S. Krowpman¹⁰⁶,
 U. Kruchonak³⁸, H. Krüger²⁴, N. Krumnack⁸⁰, M.C. Kruse⁵¹, J.A. Krzysiak⁸⁵, A. Kubota¹⁵³,
 O. Kuchinskaia³⁷, S. Kудay^{3a}, D. Kuechler⁴⁸, J.T. Kuechler⁴⁸, S. Kuehn³⁶, T. Kuhl⁴⁸,
 V. Kukhtin³⁸, Y. Kulchitsky^{37,a}, S. Kuleshov^{136d,136b}, M. Kumar^{33g}, N. Kumari¹⁰¹, A. Kupco¹³⁰,
 T. Kupfer⁴⁹, A. Kupich³⁷, O. Kuprash⁵⁴, H. Kurashige⁸³, L.L. Kurchaninov^{155a},
 Y.A. Kurochkin³⁷, A. Kurova³⁷, M. Kuze¹⁵³, A.K. Kvam¹⁰², J. Kvita¹²¹, T. Kwan¹⁰³,
 K.W. Kwok^{64a}, N.G. Kyriacou¹⁰⁵, L.A.O. Laatu¹⁰¹, C. Lacasta¹⁶², F. Lacava^{74a,74b}, H. Lacker¹⁸,
 D. Lacour¹²⁶, N.N. Lad⁹⁵, E. Ladygin³⁸, B. Laforge¹²⁶, T. Lagouri^{136e}, S. Lai⁵⁵, I.K. Lakomicz^{84a},
 N. Lalloue⁶⁰, J.E. Lambert¹¹⁹, S. Lammers⁶⁷, W. Lampl⁷, C. Lampoudis¹⁵¹, A.N. Lancaster¹¹⁴,
 E. Lançon²⁹, U. Landgraf⁵⁴, M.P.J. Landon⁹³, V.S. Lang⁵⁴, R.J. Langenberg¹⁰², A.J. Lankford¹⁵⁹,
 F. Lanni³⁶, K. Lantzsch²⁴, A. Lanza^{72a}, A. Lapertosa^{57b,57a}, J.F. Laporte¹³⁴, T. Lari^{70a},
 F. Lasagni Manghi^{23b}, M. Lassnig³⁶, V. Latonova¹³⁰, T.S. Lau^{64a}, A. Laudrain⁹⁹, A. Laurier³⁴,
 S.D. Lawlor⁹⁴, Z. Lawrence¹⁰⁰, M. Lazzaroni^{70a,70b}, B. Le¹⁰⁰, B. Leban⁹², A. Lebedev⁸⁰,
 M. LeBlanc³⁶, T. LeCompte⁶, F. Ledroit-Guillon⁶⁰, A.C.A. Lee⁹⁵, G.R. Lee¹⁶, L. Lee⁶¹,
 S.C. Lee¹⁴⁷, S. Lee^{47a,47b}, T.F. Lee⁹¹, L.L. Leeuw^{33c}, H.P. Lefebvre⁹⁴, M. Lefebvre¹⁶⁴,
 C. Leggett^{17a}, K. Lehmann¹⁴¹, G. Lehmann Miotto³⁶, M. Leigh⁵⁶, W.A. Leight¹⁰², A. Leisos^{151,u},
 M.A.L. Leite^{81c}, C.E. Leitgeb⁴⁸, R. Leitner¹³², K.J.C. Leney⁴⁴, T. Lenz²⁴, S. Leone^{73a},
 C. Leonidopoulos⁵², A. Leopold¹⁴³, C. Leroy¹⁰⁷, R. Les¹⁰⁶, C.G. Lester³², M. Levchenko³⁷,

J. Levêque⁴, D. Levin¹⁰⁵, L.J. Levinson¹⁶⁸, M.P. Lewicki⁸⁵, D.J. Lewis⁴, A. Li⁵, B. Li^{14b}, B. Li^{62b}, C. Li^{62a}, C-Q. Li^{62c}, H. Li^{62a}, H. Li^{62b}, H. Li^{14c}, H. Li^{62b}, J. Li^{62c}, K. Li¹³⁷, L. Li^{62c}, M. Li^{14a,14d}, Q.Y. Li^{62a}, S. Li^{62d,62c,e}, T. Li^{62b}, X. Li¹⁰³, Z. Li^{62b}, Z. Li¹²⁵, Z. Li¹⁰³, Z. Li⁹¹, Z. Li^{14a,14d}, Z. Liang^{14a}, M. Liberatore⁴⁸, B. Liberti^{75a}, K. Lie^{64c}, J. Lieber Marin^{81b}, K. Lin¹⁰⁶, R.A. Linck⁶⁷, R.E. Lindley⁷, J.H. Lindon², A. Linss⁴⁸, E. Lipeles¹²⁷, A. Lipniacka¹⁶, A. Lister¹⁶³, J.D. Little⁴, B. Liu^{14a}, B.X. Liu¹⁴¹, D. Liu^{62d,62c}, J.B. Liu^{62a}, J.K.K. Liu³², K. Liu^{62d,62c}, M. Liu^{62a}, M.Y. Liu^{62a}, P. Liu^{14a}, Q. Liu^{62d,137,62c}, X. Liu^{62a}, Y. Liu⁴⁸, Y. Liu^{14c,14d}, Y.L. Liu¹⁰⁵, Y.W. Liu^{62a}, M. Livan^{72a,72b}, J. Llorente Merino¹⁴¹, S.L. Lloyd⁹³, E.M. Lobodzinska⁴⁸, P. Loch⁷, S. Loffredo^{75a,75b}, T. Lohse¹⁸, K. Lohwasser¹³⁸, M. Lokajicek^{130,*}, J.D. Long¹⁶¹, I. Longarini^{74a,74b}, L. Longo^{69a,69b}, R. Longo¹⁶¹, I. Lopez Paz³⁶, A. Lopez Solis⁴⁸, J. Lorenz¹⁰⁸, N. Lorenzo Martinez⁴, A.M. Lory¹⁰⁸, A. Lösle⁵⁴, X. Lou^{47a,47b}, X. Lou^{14a,14d}, A. Lounis⁶⁶, J. Love⁶, P.A. Love⁹⁰, J.J. Lozano Bahilo¹⁶², G. Lu^{14a,14d}, M. Lu⁷⁹, S. Lu¹²⁷, Y.J. Lu⁶⁵, H.J. Lubatti¹³⁷, C. Luci^{74a,74b}, F.L. Lucio Alves^{14c}, A. Lucotte⁶⁰, F. Luehring⁶⁷, I. Luise¹⁴⁴, O. Lukianchuk⁶⁶, O. Lundberg¹⁴³, B. Lund-Jensen¹⁴³, N.A. Luongo¹²², M.S. Lutz¹⁵⁰, D. Lynn²⁹, H. Lyons⁹¹, R. Lysak¹³⁰, E. Lytken⁹⁷, F. Lyu^{14a}, V. Lyubushkin³⁸, T. Lyubushkina³⁸, H. Ma²⁹, L.L. Ma^{62b}, Y. Ma⁹⁵, D.M. Mac Donell¹⁶⁴, G. Maccarrone⁵³, J.C. MacDonald¹³⁸, R. Madar⁴⁰, W.F. Mader⁵⁰, J. Maeda⁸³, T. Maeno²⁹, M. Maerker⁵⁰, V. Magerl⁵⁴, J. Magro^{68a,68c}, H. Maguire¹³⁸, D.J. Mahon⁴¹, C. Maidantchik^{81b}, A. Maio^{129a,129b,129d}, K. Maj^{84a}, O. Majersky^{28a}, S. Majewski¹²², N. Makovec⁶⁶, V. Maksimovic¹⁵, B. Malaescu¹²⁶, Pa. Malecki⁸⁵, V.P. Maleev³⁷, F. Malek⁶⁰, D. Malito^{43b,43a}, U. Mallik⁷⁹, C. Malone³², S. Maltezos¹⁰, S. Malyukov³⁸, J. Mamuzic¹³, G. Mancini⁵³, G. Manco^{72a,72b}, J.P. Mandalia⁹³, I. Mandić⁹², L. Manhaes de Andrade Filho^{81a}, I.M. Maniatis¹⁵¹, M. Manisha¹³⁴, J. Manjarres Ramos⁵⁰, D.C. Mankad¹⁶⁸, A. Mann¹⁰⁸, B. Mansoulie¹³⁴, S. Manzoni³⁶, A. Marantis^{151,u}, G. Marchiori⁵, M. Marcisovsky¹³⁰, L. Marcoccia^{75a,75b}, C. Marcon^{70a,70b}, M. Marinescu²⁰, M. Marjanovic¹¹⁹, Z. Marshall^{17a}, S. Marti-Garcia¹⁶², T.A. Martin¹⁶⁶, V.J. Martin⁵², B. Martin dit Latour¹⁶, L. Martinelli^{74a,74b}, M. Martinez^{13,v}, P. Martinez Agullo¹⁶², V.I. Martinez Outschoorn¹⁰², P. Martinez Suarez¹³, S. Martin-Haugh¹³³, V.S. Martoiu^{27b}, A.C. Martyniuk⁹⁵, A. Marzin³⁶, S.R. Maschek¹⁰⁹, L. Masetti⁹⁹, T. Mashimo¹⁵², J. Masik¹⁰⁰, A.L. Maslennikov³⁷, L. Massa^{23b}, P. Massarotti^{71a,71b}, P. Mastrandrea^{73a,73b}, A. Mastroberardino^{43b,43a}, T. Masubuchi¹⁵², T. Mathisen¹⁶⁰, N. Matsuzawa¹⁵², J. Maurer^{27b}, B. Maček⁹², D.A. Maximov³⁷, R. Mazini¹⁴⁷, I. Maznas¹⁵¹, M. Mazza¹⁰⁶, S.M. Mazza¹³⁵, C. Mc Ginn²⁹, J.P. Mc Gowan¹⁰³, S.P. Mc Kee¹⁰⁵, W.P. McCormack^{17a}, E.F. McDonald¹⁰⁴, A.E. McDougall¹¹³, J.A. Mcfayden¹⁴⁵, G. Mchedlidze^{148b}, R.P. Mckenzie^{33g}, T.C. Mclachlan⁴⁸, D.J. Mclaughlin⁹⁵, K.D. McLean¹⁶⁴, S.J. McMahan¹³³, P.C. McNamara¹⁰⁴, C.M. Mcpartland⁹¹, R.A. McPherson^{164,y}, T. Megy⁴⁰, S. Mehlhase¹⁰⁸, A. Mehta⁹¹, B. Meirose⁴⁵, D. Melini¹⁴⁹, B.R. Mellado Garcia^{33g}, A.H. Melo⁵⁵, F. Meloni⁴⁸, E.D. Mendes Gouveia^{129a}, A.M. Mendes Jacques Da Costa²⁰, H.Y. Meng¹⁵⁴, L. Meng⁹⁰, S. Menke¹⁰⁹, M. Mentink³⁶, E. Meoni^{43b,43a}, C. Merlassino¹²⁵, L. Merola^{71a,71b}, C. Meroni^{70a}, G. Merz¹⁰⁵, O. Meshkov³⁷, J.K.R. Meshreki¹⁴⁰, J. Metcalfe⁶, A.S. Mete⁶, C. Meyer⁶⁷, J-P. Meyer¹³⁴, M. Michetti¹⁸, R.P. Middleton¹³³, L. Mijović⁵², G. Mikenberg¹⁶⁸, M. Míkestikova¹³⁰, M. Mikuž⁹², H. Mildner¹³⁸, A. Milic³⁶, C.D. Milke⁴⁴, D.W. Miller³⁹, L.S. Miller³⁴, A. Milov¹⁶⁸, D.A. Milstead^{47a,47b}, T. Min^{14c}, A.A. Minaenko³⁷, I.A. Minashvili^{148b}, L. Mince⁵⁹, A.I. Mincer¹¹⁶, B. Mindur^{84a}, M. Mineev³⁸, Y. Mino⁸⁶, L.M. Mir¹³, M. Miralles Lopez¹⁶², M. Mironova¹²⁵, M.C. Missio¹¹², T. Mitani¹⁶⁷, A. Mitra¹⁶⁶,

V.A. Mitsou¹⁶², O. Miu¹⁵⁴, P.S. Miyagawa⁹³, Y. Miyazaki⁸⁸, A. Mizukami⁸², J.U. Mjörnmark⁹⁷, T. Mkrtchyan^{63a}, T. Mlinarevic⁹⁵, M. Mlynarikova³⁶, T. Moa^{47a,47b}, S. Mobius⁵⁵, K. Mochizuki¹⁰⁷, P. Moder⁴⁸, P. Mogg¹⁰⁸, A.F. Mohammed^{14a,14d}, S. Mohapatra⁴¹, G. Mokgatitswane^{33g}, B. Mondal¹⁴⁰, S. Mondal¹³¹, K. Mönig⁴⁸, E. Monnier¹⁰¹, L. Monsonis Romero¹⁶², J. Montejo Berlingen³⁶, M. Montella¹¹⁸, F. Monticelli⁸⁹, N. Morange⁶⁶, A.L. Moreira De Carvalho^{129a}, M. Moreno Llácer¹⁶², C. Moreno Martinez⁵⁶, P. Morettini^{57b}, S. Morgenstern¹⁶⁶, M. Morii⁶¹, M. Morinaga¹⁵², V. Morisbak¹²⁴, A.K. Morley³⁶, F. Morodei^{74a,74b}, L. Morvaj³⁶, P. Moschovakos³⁶, B. Moser³⁶, M. Mosidze^{148b}, T. Moskalets⁵⁴, P. Moskvitina¹¹², J. Moss^{31,o}, E.J.W. Moyse¹⁰², S. Muanza¹⁰¹, J. Mueller¹²⁸, D. Muenstermann⁹⁰, R. Müller¹⁹, G.A. Mullier⁹⁷, J.J. Mullin¹²⁷, D.P. Mungo¹⁵⁴, J.L. Munoz Martinez¹³, D. Munoz Perez¹⁶², F.J. Munoz Sanchez¹⁰⁰, M. Murin¹⁰⁰, W.J. Murray^{166,133}, A. Murrone^{70a,70b}, J.M. Muse¹¹⁹, M. Muškinja^{17a}, C. Mwewa²⁹, A.G. Myagkov^{37,a}, A.J. Myers⁸, A.A. Myers¹²⁸, G. Myers⁶⁷, M. Myska¹³¹, B.P. Nachman^{17a}, O. Nackenhorst⁴⁹, A. Nag⁵⁰, K. Nagai¹²⁵, K. Nagano⁸², J.L. Nagle^{29,al}, E. Nagy¹⁰¹, A.M. Nairz³⁶, Y. Nakahama⁸², K. Nakamura⁸², H. Nanjo¹²³, R. Narayan⁴⁴, E.A. Narayanan¹¹¹, I. Naryshkin³⁷, M. Naseri³⁴, C. Nass²⁴, G. Navarro^{22a}, J. Navarro-Gonzalez¹⁶², R. Nayak¹⁵⁰, A. Nayaz¹⁸, P.Y. Nechaeva³⁷, F. Nechansky⁴⁸, L. Nedic¹²⁵, T.J. Neep²⁰, A. Negri^{72a,72b}, M. Negrini^{23b}, C. Nellist¹¹², C. Nelson¹⁰³, K. Nelson¹⁰⁵, S. Nemecek¹³⁰, M. Nessi^{36,h}, M.S. Neubauer¹⁶¹, F. Neuhaus⁹⁹, J. Neundorfer⁴⁸, R. Newhouse¹⁶³, P.R. Newman²⁰, C.W. Ng¹²⁸, Y.S. Ng¹⁸, Y.W.Y. Ng⁴⁸, B. Ngair^{35e}, H.D.N. Nguyen¹⁰⁷, R.B. Nickerson¹²⁵, R. Nicolaidou¹³⁴, J. Nielsen¹³⁵, M. Niemeyer⁵⁵, N. Nikiforou³⁶, V. Nikolaenko^{37,a}, I. Nikolic-Audit¹²⁶, K. Nikolopoulos²⁰, P. Nilsson²⁹, H.R. Nindhito⁵⁶, A. Nisati^{74a}, N. Nishu², R. Nisius¹⁰⁹, J-E. Nitschke⁵⁰, E.K. Nkadimeng^{33g}, S.J. Noacco Rosende⁸⁹, T. Nobe¹⁵², D.L. Noel³², Y. Noguchi⁸⁶, T. Nommensen¹⁴⁶, M.A. Nomura²⁹, M.B. Norfolk¹³⁸, R.R.B. Norisam⁹⁵, B.J. Norman³⁴, J. Novak⁹², T. Novak⁴⁸, O. Novgorodova⁵⁰, L. Novotny¹³¹, R. Novotny¹¹¹, L. Nozka¹²¹, K. Ntekas¹⁵⁹, N.M.J. Nunes De Moura Junior^{81b}, E. Nurse⁹⁵, F.G. Oakham^{34,ai}, J. Ocariz¹²⁶, A. Ochi⁸³, I. Ochoa^{129a}, S. Oerdek¹⁶⁰, A. Ogrodnik^{84a}, A. Oh¹⁰⁰, C.C. Ohm¹⁴³, H. Oide¹⁵³, R. Oishi¹⁵², M.L. Ojeda⁴⁸, Y. Okazaki⁸⁶, M.W. O'Keefe⁹¹, Y. Okumura¹⁵², A. Olariu^{27b}, L.F. Oleiro Seabra^{129a}, S.A. Olivares Pino^{136e}, D. Oliveira Damazio²⁹, D. Oliveira Goncalves^{81a}, J.L. Oliver¹⁵⁹, M.J.R. Olsson¹⁵⁹, A. Olszewski⁸⁵, J. Olszowska^{85,*}, Ö.O. Öncel⁵⁴, D.C. O'Neil¹⁴¹, A.P. O'Neill¹⁹, A. Onofre^{129a,129e}, P.U.E. Onyisi¹¹, M.J. Oreglia³⁹, G.E. Orellana⁸⁹, D. Orestano^{76a,76b}, N. Orlando¹³, R.S. Orr¹⁵⁴, V. O'Shea⁵⁹, R. Ospanov^{62a}, G. Otero y Garzon³⁰, H. Otono⁸⁸, P.S. Ott^{63a}, G.J. Ottino^{17a}, M. Ouchrif^{35d}, J. Ouellette^{29,al}, F. Ould-Saada¹²⁴, M. Owen⁵⁹, R.E. Owen¹³³, K.Y. Oyulmaz^{21a}, V.E. Ozcan^{21a}, N. Ozturk⁸, S. Ozturk^{21d}, J. Pacalt¹²¹, H.A. Pacey³², K. Pachal⁵¹, A. Pacheco Pages¹³, C. Padilla Aranda¹³, G. Padovano^{74a,74b}, S. Pagan Griso^{17a}, G. Palacino⁶⁷, A. Palazzo^{69a,69b}, S. Palazzo⁵², S. Palestini³⁶, M. Palka^{84b}, J. Pan¹⁷¹, T. Pan^{64a}, D.K. Panchal¹¹, C.E. Pandini¹¹³, J.G. Panduro Vazquez⁹⁴, H. Pang^{14b}, P. Pani⁴⁸, G. Panizzo^{68a,68c}, L. Paolozzi⁵⁶, C. Papadatos¹⁰⁷, S. Parajuli⁴⁴, A. Paramonov⁶, C. Paraskevopoulos¹⁰, D. Paredes Hernandez^{64b}, T.H. Park¹⁵⁴, M.A. Parker³², F. Parodi^{57b,57a}, E.W. Parrish¹¹⁴, V.A. Parrish⁵², J.A. Parsons⁴¹, U. Parzefall⁵⁴, B. Pascual Dias¹⁰⁷, L. Pascual Dominguez¹⁵⁰, V.R. Pascuzzi^{17a}, F. Pasquali¹¹³, E. Pasqualucci^{74a}, S. Passaggio^{57b}, F. Pastore⁹⁴, P. Pasuwan^{47a,47b}, P. Patel⁸⁵, J.R. Pater¹⁰⁰, J. Patton⁹¹, T. Pauly³⁶, J. Parkes¹⁴², M. Pedersen¹²⁴, R. Pedro^{129a}, S.V. Peleganchuk³⁷, O. Penc³⁶, E.A. Pender⁵²,

C. Peng^{64b}, H. Peng^{62a}, K.E. Penski¹⁰⁸, M. Penzin³⁷, B.S. Peralva^{81d}, A.P. Pereira Peixoto⁶⁰,
 L. Pereira Sanchez^{47a,47b}, D.V. Perepelitsa^{29,al}, E. Perez Codina^{155a}, M. Perganti¹⁰,
 L. Perini^{70a,70b,*}, H. Pernegger³⁶, S. Perrella³⁶, A. Perrevoort¹¹², O. Perrin⁴⁰, K. Peters⁴⁸,
 R.F.Y. Peters¹⁰⁰, B.A. Petersen³⁶, T.C. Petersen⁴², E. Petit¹⁰¹, V. Petousis¹³¹, C. Petridou¹⁵¹,
 A. Petrukhin¹⁴⁰, M. Pettee^{17a}, N.E. Pettersson³⁶, A. Petukhov³⁷, K. Petukhova¹³², A. Peyaud¹³⁴,
 R. Pezoa^{136f}, L. Pezzotti³⁶, G. Pezzullo¹⁷¹, T.M. Pham¹⁶⁹, T. Pham¹⁰⁴, P.W. Phillips¹³³,
 M.W. Phipps¹⁶¹, G. Piacquadio¹⁴⁴, E. Pianori^{17a}, F. Piazza^{70a,70b}, R. Piegaia³⁰, D. Pietreanu^{27b},
 A.D. Pilkington¹⁰⁰, M. Pinamonti^{68a,68c}, J.L. Pinfeld², B.C. Pinheiro Pereira^{129a},
 C. Pitman Donaldson⁹⁵, D.A. Pizzi³⁴, L. Pizzimento^{75a,75b}, A. Pizzini¹¹³, M.-A. Pleier²⁹,
 V. Plesanovs⁵⁴, V. Pleskot¹³², E. Plotnikova³⁸, G. Poddar⁴, R. Poettgen⁹⁷, L. Poggioli¹²⁶,
 I. Pogrebnyak¹⁰⁶, D. Pohl²⁴, I. Pokharel⁵⁵, S. Polacek¹³², G. Polesello^{72a}, A. Poley^{141,155a},
 R. Polifka¹³¹, A. Polini^{23b}, C.S. Pollard¹²⁵, Z.B. Pollock¹¹⁸, V. Polychronakos²⁹,
 E. Pompa Pacchi^{74a,74b}, D. Ponomarenko³⁷, L. Pontecorvo³⁶, S. Popa^{27a}, G.A. Popeneciu^{27d},
 D.M. Portillo Quintero^{155a}, S. Pospisil¹³¹, P. Postolache^{27c}, K. Potamianos¹²⁵, I.N. Potrap³⁸,
 C.J. Potter³², H. Potti¹, T. Poulsen⁴⁸, J. Poveda¹⁶², M.E. Pozo Astigarraga³⁶, A. Prades Ibanez¹⁶²,
 M.M. Prapa⁴⁶, J. Pretel⁵⁴, D. Price¹⁰⁰, M. Primavera^{69a}, M.A. Principe Martin⁹⁸, R. Privara¹²¹,
 M.L. Proffitt¹³⁷, N. Proklova¹²⁷, K. Prokofiev^{64c}, G. Proto^{75a,75b}, S. Protopopescu²⁹,
 J. Proudfoot⁶, M. Przybycien^{84a}, J.E. Puddefoot¹³⁸, D. Pudzha³⁷, P. Puzo⁶⁶, D. Pyatiizbyantseva³⁷,
 J. Qian¹⁰⁵, D. Qichen¹⁰⁰, Y. Qin¹⁰⁰, T. Qiu⁹³, A. Quadt⁵⁵, M. Queitsch-Maitland¹⁰⁰,
 G. Quetant⁵⁶, G. Rabanal Bolanos⁶¹, D. Rafanoharana⁵⁴, F. Ragusa^{70a,70b}, J.L. Rainbolt³⁹,
 J.A. Raine⁵⁶, S. Rajagopalan²⁹, E. Ramakoti³⁷, K. Ran^{48,14d}, N.P. Rapheeha^{33g}, V. Raskina¹²⁶,
 D.F. Rassloff^{63a}, S. Rave⁹⁹, B. Ravina⁵⁵, I. Ravinovich¹⁶⁸, M. Raymond³⁶, A.L. Read¹²⁴,
 N.P. Readioff¹³⁸, D.M. Rebuzzi^{72a,72b}, G. Redlinger²⁹, K. Reeves⁴⁵, J.A. Reidelsturz¹⁷⁰,
 D. Reikher¹⁵⁰, A. Reiss⁹⁹, A. Rej¹⁴⁰, C. Rembser³⁶, A. Renardi⁴⁸, M. Renda^{27b}, M.B. Rendel¹⁰⁹,
 F. Renner⁴⁸, A.G. Rennie⁵⁹, S. Resconi^{70a}, M. Ressegotti^{57b,57a}, E.D. Resseguie^{17a}, S. Rettie³⁶,
 B. Reynolds¹¹⁸, E. Reynolds^{17a}, M. Rezaei Estabragh¹⁷⁰, O.L. Rezanova³⁷, P. Reznicek¹³²,
 E. Ricci^{77a,77b}, R. Richter¹⁰⁹, S. Richter^{47a,47b}, E. Richter-Was^{84b}, M. Ridel¹²⁶, P. Rieck¹¹⁶,
 P. Riedler³⁶, M. Rijssenbeek¹⁴⁴, A. Rimoldi^{72a,72b}, M. Rimoldi⁴⁸, L. Rinaldi^{23b,23a}, T.T. Rinn²⁹,
 M.P. Rinnagel¹⁰⁸, G. Ripellino¹⁴³, I. Riu¹³, P. Rivadeneira⁴⁸, J.C. Rivera Vergara¹⁶⁴,
 F. Rizatdinova¹²⁰, E. Rizvi⁹³, C. Rizzi⁵⁶, B.A. Roberts¹⁶⁶, B.R. Roberts^{17a}, S.H. Robertson^{103,y},
 M. Robin⁴⁸, D. Robinson³², C.M. Robles Gajardo^{136f}, M. Robles Manzano⁹⁹, A. Robson⁵⁹,
 A. Rocchi^{75a,75b}, C. Roda^{73a,73b}, S. Rodriguez Bosca^{63a}, Y. Rodriguez Garcia^{22a},
 A. Rodriguez Rodriguez⁵⁴, A.M. Rodríguez Vera^{155b}, S. Roe³⁶, J.T. Roemer¹⁵⁹,
 A.R. Roepe-Gier¹¹⁹, J. Roggel¹⁷⁰, O. Røhne¹²⁴, R.A. Rojas¹⁶⁴, B. Roland⁵⁴, C.P.A. Roland⁶⁷,
 J. Roloff²⁹, A. Romaniouk³⁷, E. Romano^{72a,72b}, M. Romano^{23b}, A.C. Romero Hernandez¹⁶¹,
 N. Rompotis⁹¹, L. Roos¹²⁶, S. Rosati^{74a}, B.J. Rosser³⁹, E. Rossi⁴, E. Rossi^{71a,71b}, L.P. Rossi^{57b},
 L. Rossini⁴⁸, R. Rosten¹¹⁸, M. Rotaru^{27b}, B. Rottler⁵⁴, D. Rousseau⁶⁶, D. Rousso³²,
 G. Rovelli^{72a,72b}, A. Roy¹⁶¹, A. Rozanov¹⁰¹, Y. Rozen¹⁴⁹, X. Ruan^{33g}, A. Rubio Jimenez¹⁶²,
 A.J. Ruby⁹¹, V.H. Ruelas Rivera¹⁸, T.A. Ruggeri¹, F. Rühr⁵⁴, A. Ruiz-Martinez¹⁶², A. Rummler³⁶,
 Z. Rurikova⁵⁴, N.A. Rusakovich³⁸, H.L. Russell¹⁶⁴, J.P. Rutherford⁷, K. Rybacki⁹⁰, M. Rybar¹³²,
 E.B. Rye¹²⁴, A. Ryzhov³⁷, J.A. Sabater Iglesias⁵⁶, P. Sabatini¹⁶², L. Sabetta^{74a,74b},
 H.F.W. Sadrozinski¹³⁵, F. Safai Tehrani^{74a}, B. Safarzadeh Samani¹⁴⁵, M. Safdari¹⁴², S. Saha¹⁰³,
 M. Sahinsoy¹⁰⁹, M. Saimpert¹³⁴, M. Saito¹⁵², T. Saito¹⁵², D. Salamani³⁶, G. Salamanna^{76a,76b},

A. Salnikov¹⁴², J. Salt¹⁶², A. Salvador Salas¹³, D. Salvatore^{43b,43a}, F. Salvatore¹⁴⁵,
 A. Salzburger³⁶, D. Sammel⁵⁴, D. Sampsonidis¹⁵¹, D. Sampsonidou^{62d,62c}, J. Sánchez¹⁶²,
 A. Sanchez Pineda⁴, V. Sanchez Sebastian¹⁶², H. Sandaker¹²⁴, C.O. Sander⁴⁸, J.A. Sandesara¹⁰²,
 M. Sandhoff¹⁷⁰, C. Sandoval^{22b}, D.P.C. Sankey¹³³, A. Sansoni⁵³, L. Santi^{74a,74b}, C. Santoni⁴⁰,
 H. Santos^{129a,129b}, S.N. Santpur^{17a}, A. Santra¹⁶⁸, K.A. Saoucha¹³⁸, J.G. Saraiva^{129a,129d},
 J. Sardain⁷, O. Sasaki⁸², K. Sato¹⁵⁶, C. Sauer^{63b}, F. Sauerburger⁵⁴, E. Sauvan⁴, P. Savard^{154,ai},
 R. Sawada¹⁵², C. Sawyer¹³³, L. Sawyer⁹⁶, I. Sayago Galvan¹⁶², C. Sbarra^{23b}, A. Sbrizzi^{23b,23a},
 T. Scanlon⁹⁵, J. Schaarschmidt¹³⁷, P. Schacht¹⁰⁹, D. Schaefer³⁹, U. Schäfer⁹⁹, A.C. Schaffer⁶⁶,
 D. Schaile¹⁰⁸, R.D. Schamberger¹⁴⁴, E. Schanet¹⁰⁸, C. Scharf¹⁸, M.M. Schefer¹⁹,
 V.A. Schegelsky³⁷, D. Scheirich¹³², F. Schenk¹⁸, M. Schernau¹⁵⁹, C. Scheulen⁵⁵,
 C. Schiavi^{57b,57a}, Z.M. Schillaci²⁶, E.J. Schioppa^{69a,69b}, M. Schioppa^{43b,43a}, B. Schlag⁹⁹,
 K.E. Schleicher⁵⁴, S. Schlenker³⁶, M.A. Schmidt¹⁷⁰, K. Schmieden⁹⁹, C. Schmitt⁹⁹, S. Schmitt⁴⁸,
 L. Schoeffel¹³⁴, A. Schoening^{63b}, P.G. Scholer⁵⁴, E. Schopf¹²⁵, M. Schott⁹⁹, J. Schovancova³⁶,
 S. Schramm⁵⁶, F. Schroeder¹⁷⁰, H-C. Schultz-Coulon^{63a}, M. Schumacher⁵⁴, B.A. Schumm¹³⁵,
 Ph. Schune¹³⁴, A. Schwartzman¹⁴², T.A. Schwarz¹⁰⁵, Ph. Schwemling¹³⁴, R. Schwienhorst¹⁰⁶,
 A. Sciandra¹³⁵, G. Sciolla²⁶, F. Scuri^{73a}, F. Scutti¹⁰⁴, C.D. Sebastiani⁹¹, K. Sedlaczek⁴⁹,
 P. Seema¹⁸, S.C. Seidel¹¹¹, A. Seiden¹³⁵, B.D. Seidlitz⁴¹, T. Seiss³⁹, C. Seitz⁴⁸, J.M. Seixas^{81b},
 G. Sekhniaidze^{71a}, S.J. Sekula⁴⁴, L. Selem⁴, N. Semprini-Cesari^{23b,23a}, S. Sen⁵¹, D. Sengupta⁵⁶,
 V. Senthilkumar¹⁶², L. Serin⁶⁶, L. Serkin^{68a,68b}, M. Sessa^{76a,76b}, H. Severini¹¹⁹, S. Sevova¹⁴²,
 F. Sforza^{57b,57a}, A. Sfyrila⁵⁶, E. Shabalina⁵⁵, R. Shaheen¹⁴³, J.D. Shahinian¹²⁷, N.W. Shaikh^{47a,47b},
 D. Shaked Renous¹⁶⁸, L.Y. Shan^{14a}, M. Shapiro^{17a}, A. Sharma³⁶, A.S. Sharma¹⁶³, P. Sharma⁷⁹,
 S. Sharma⁴⁸, P.B. Shatalov³⁷, K. Shaw¹⁴⁵, S.M. Shaw¹⁰⁰, Q. Shen^{62c,5}, P. Sherwood⁹⁵, L. Shi⁹⁵,
 C.O. Shimmin¹⁷¹, Y. Shimogama¹⁶⁷, J.D. Shinner⁹⁴, I.P.J. Shipsey¹²⁵, S. Shirabe⁶⁰,
 M. Shiyakova^{38,x}, J. Shlomi¹⁶⁸, M.J. Shochet³⁹, J. Shojaii¹⁰⁴, D.R. Shope¹²⁴, S. Shrestha^{118,am},
 E.M. Shrif^{33g}, M.J. Shroff¹⁶⁴, P. Sicho¹³⁰, A.M. Sickles¹⁶¹, E. Sideras Haddad^{33g}, A. Sidoti^{23b},
 F. Siegert⁵⁰, Dj. Sijacki¹⁵, R. Sikora^{84a}, F. Sili⁸⁹, J.M. Silva²⁰, M.V. Silva Oliveira³⁶,
 S.B. Silverstein^{47a}, S. Simion⁶⁶, R. Simoniello³⁶, E.L. Simpson⁵⁹, N.D. Simpson⁹⁷, S. Simsek^{21d},
 S. Sindhu⁵⁵, P. Sinervo¹⁵⁴, V. Sinetckii³⁷, S. Singh¹⁴¹, S. Singh¹⁵⁴, S. Sinha⁴⁸, S. Sinha^{33g},
 M. Sioli^{23b,23a}, I. Siral³⁶, S.Yu. Sivoklov^{37,*}, J. Sjölin^{47a,47b}, A. Skaf⁵⁵, E. Skorda⁹⁷,
 P. Skubic¹¹⁹, M. Slawinska⁸⁵, V. Smakhtin¹⁶⁸, B.H. Smart¹³³, J. Smiesko³⁶, S.Yu. Smirnov³⁷,
 Y. Smirnov³⁷, L.N. Smirnova^{37,a}, O. Smirnova⁹⁷, A.C. Smith⁴¹, E.A. Smith³⁹, H.A. Smith¹²⁵,
 J.L. Smith⁹¹, R. Smith¹⁴², M. Smizanska⁹⁰, K. Smolek¹³¹, A. Smykiewicz⁸⁵, A.A. Snesarev³⁷,
 H.L. Snoek¹¹³, S. Snyder²⁹, R. Sobie^{164,y}, A. Soffer¹⁵⁰, C.A. Solans Sanchez³⁶, E.Yu. Soldatov³⁷,
 U. Soldevila¹⁶², A.A. Solodkov³⁷, S. Solomon⁵⁴, A. Soloshenko³⁸, K. Solovieva⁵⁴,
 O.V. Solovyanov³⁷, V. Solovyev³⁷, P. Sommer³⁶, A. Sonay¹³, W.Y. Song^{155b}, A. Sopczak¹³¹,
 A.L. Soppio⁹⁵, F. Sopkova^{28b}, V. Sothilingam^{63a}, S. Sottocornola^{72a,72b}, R. Soualah^{115b},
 Z. Soumami^{35e}, D. South⁴⁸, S. Spagnolo^{69a,69b}, M. Spalla¹⁰⁹, F. Spanò⁹⁴, D. Sperlich⁵⁴,
 G. Spigo³⁶, M. Spina¹⁴⁵, S. Spinali⁹⁰, D.P. Spiteri⁵⁹, M. Spousta¹³², E.J. Staats³⁴,
 A. Stabile^{70a,70b}, R. Stamen^{63a}, M. Stamenkovic¹¹³, A. Stampekis²⁰, M. Standke²⁴, E. Stanecka⁸⁵,
 M.V. Stange⁵⁰, B. Stanislaus^{17a}, M.M. Stanitzki⁴⁸, M. Stankaityte¹²⁵, B. Stapf⁴⁸,
 E.A. Starchenko³⁷, G.H. Stark¹³⁵, J. Stark^{101,ac}, D.M. Starke^{155b}, P. Staroba¹³⁰, P. Starovoitov^{63a},
 S. Stärz¹⁰³, R. Staszewski⁸⁵, G. Stavropoulos⁴⁶, J. Steentoft¹⁶⁰, P. Steinberg²⁹, A.L. Steinhebel¹²²,
 B. Stelzer^{141,155a}, H.J. Stelzer¹²⁸, O. Stelzer-Chilton^{155a}, H. Stenzel⁵⁸, T.J. Stevenson¹⁴⁵,

G.A. Stewart³⁶, M.C. Stockton³⁶, G. Stoicea^{27b}, M. Stolarski^{129a}, S. Stonjek¹⁰⁹, A. Straessner⁵⁰, J. Strandberg¹⁴³, S. Strandberg^{47a,47b}, M. Strauss¹¹⁹, T. Strebler¹⁰¹, P. Strizenec^{28b}, R. Ströhmer¹⁶⁵, D.M. Strom¹²², L.R. Strom⁴⁸, R. Stroynowski⁴⁴, A. Strubig^{47a,47b}, S.A. Stucci²⁹, B. Stugu¹⁶, J. Stupak¹¹⁹, N.A. Styles⁴⁸, D. Su¹⁴², S. Su^{62a}, W. Su^{62d,137,62c}, X. Su^{62a,66}, K. Sugizaki¹⁵², V.V. Sulin³⁷, M.J. Sullivan⁹¹, D.M.S. Sultan^{77a,77b}, L. Sultanaliyeva³⁷, S. Sultansoy^{3b}, T. Sumida⁸⁶, S. Sun¹⁰⁵, S. Sun¹⁶⁹, O. Sunneborn Gudnadottir¹⁶⁰, M.R. Sutton¹⁴⁵, M. Svatos¹³⁰, M. Swiatlowski^{155a}, T. Swirski¹⁶⁵, I. Sykora^{28a}, M. Sykora¹³², T. Sykora¹³², D. Ta⁹⁹, K. Tackmann^{48,w}, A. Taffard¹⁵⁹, R. Tafirout^{155a}, J.S. Tafoya Vargas⁶⁶, R.H.M. Taibah¹²⁶, R. Takashima⁸⁷, K. Takeda⁸³, E.P. Takeva⁵², Y. Takubo⁸², M. Talby¹⁰¹, A.A. Talyshv³⁷, K.C. Tam^{64b}, N.M. Tamir¹⁵⁰, A. Tanaka¹⁵², J. Tanaka¹⁵², R. Tanaka⁶⁶, M. Tanasini^{57b,57a}, J. Tang^{62c}, Z. Tao¹⁶³, S. Tapia Araya⁸⁰, S. Tapprogge⁹⁹, A. Tarek Abouelfadl Mohamed¹⁰⁶, S. Tarem¹⁴⁹, K. Tariq^{62b}, G. Tarna^{101,27b}, G.F. Tartarelli^{70a}, P. Tas¹³², M. Tasevsky¹³⁰, E. Tassi^{43b,43a}, A.C. Tate¹⁶¹, G. Tateno¹⁵², Y. Tayalati^{35e}, G.N. Taylor¹⁰⁴, W. Taylor^{155b}, H. Teagle⁹¹, A.S. Tee¹⁶⁹, R. Teixeira De Lima¹⁴², P. Teixeira-Dias⁹⁴, J.J. Teoh¹⁵⁴, K. Terashi¹⁵², J. Terron⁹⁸, S. Terzo¹³, M. Testa⁵³, R.J. Teuscher^{154,y}, A. Thaler⁷⁸, O. Theiner⁵⁶, N. Themistokleous⁵², T. Thevenaux-Pelzer¹⁸, O. Thielmann¹⁷⁰, D.W. Thomas⁹⁴, J.P. Thomas²⁰, E.A. Thompson⁴⁸, P.D. Thompson²⁰, E. Thomson¹²⁷, E.J. Thorpe⁹³, Y. Tian⁵⁵, V. Tikhomirov^{37,a}, Yu.A. Tikhonov³⁷, S. Timoshenko³⁷, E.X.L. Ting¹, P. Tipton¹⁷¹, S. Tisserant¹⁰¹, S.H. Tlou^{33g}, A. Tnourji⁴⁰, K. Todome^{23b,23a}, S. Todorova-Nova¹³², S. Todt⁵⁰, M. Togawa⁸², J. Tojo⁸⁸, S. Tokár^{28a}, K. Tokushuku⁸², R. Tombs³², M. Tomoto^{82,110}, L. Tompkins^{142,q}, K.W. Topolnicki^{84b}, P. Tornambe¹⁰², E. Torrence¹²², H. Torres⁵⁰, E. Torró Pastor¹⁶², M. Toscani³⁰, C. Toscirri³⁹, D.R. Tovey¹³⁸, A. Traeet¹⁶, I.S. Trandafir^{27b}, T. Trefzger¹⁶⁵, A. Tricoli²⁹, I.M. Trigger^{155a}, S. Trincaz-Duvoid¹²⁶, D.A. Trischuk²⁶, B. Trocmé⁶⁰, A. Trofymov⁶⁶, C. Troncon^{70a}, L. Truong^{33c}, M. Trzebinski⁸⁵, A. Trzupiek⁸⁵, F. Tsai¹⁴⁴, M. Tsai¹⁰⁵, A. Tsiamis¹⁵¹, P.V. Tsiarehka³⁷, S. Tsigaridas^{155a}, A. Tsirigotis^{151,u}, V. Tsiskaridze¹⁴⁴, E.G. Tskhadadze^{148a}, M. Tsooulou¹⁵¹, Y. Tsujikawa⁸⁶, I.I. Tsukerman³⁷, V. Tsulaia^{17a}, S. Tsuno⁸², O. Tsur¹⁴⁹, D. Tsybychev¹⁴⁴, Y. Tu^{64b}, A. Tudorache^{27b}, V. Tudorache^{27b}, A.N. Tuna³⁶, S. Turchikhin³⁸, I. Turk Cakir^{3a}, R. Turra^{70a}, T. Turtuvshin^{38,z}, P.M. Tuts⁴¹, S. Tzamarias¹⁵¹, P. Tzanis¹⁰, E. Tzovara⁹⁹, K. Uchida¹⁵², F. Ukegawa¹⁵⁶, P.A. Ulloa Poblete^{136c}, G. Unal³⁶, M. Unal¹¹, A. Undrus²⁹, G. Unel¹⁵⁹, J. Urban^{28b}, P. Urquijo¹⁰⁴, G. Usai⁸, R. Ushioda¹⁵³, M. Usman¹⁰⁷, Z. Uysal^{21b}, V. Vacek¹³¹, B. Vachon¹⁰³, K.O.H. Vadla¹²⁴, T. Vafeiadis³⁶, C. Valderanis¹⁰⁸, E. Valdes Santurio^{47a,47b}, M. Valente^{155a}, S. Valentinetti^{23b,23a}, A. Valero¹⁶², A. Vallier^{101,ac}, J.A. Valls Ferrer¹⁶², T.R. Van Daalen¹³⁷, P. Van Gemmeren⁶, M. Van Rijnbach^{124,36}, S. Van Stroud⁹⁵, I. Van Vulpen¹¹³, M. Vanadia^{75a,75b}, W. Vandelli³⁶, M. Vandenbroucke¹³⁴, E.R. Vandewall¹²⁰, D. Vannicola¹⁵⁰, L. Vannoli^{57b,57a}, R. Vari^{74a}, E.W. Varnes⁷, C. Varni^{17a}, T. Varol¹⁴⁷, D. Varouchas⁶⁶, L. Varriale¹⁶², K.E. Varvell¹⁴⁶, M.E. Vasile^{27b}, L. Vaslin⁴⁰, G.A. Vasquez¹⁶⁴, F. Vazeille⁴⁰, T. Vazquez Schroeder³⁶, J. Veatch³¹, V. Vecchio¹⁰⁰, M.J. Veen¹⁰², I. Velisek¹²⁵, L.M. Veloce¹⁵⁴, F. Veloso^{129a,129c}, S. Veneziano^{74a}, A. Ventura^{69a,69b}, A. Verbytskyi¹⁰⁹, M. Verducci^{73a,73b}, C. Vergis²⁴, M. Verissimo De Araujo^{81b}, W. Verkerke¹¹³, J.C. Vermeulen¹¹³, C. Vernieri¹⁴², P.J. Verschuuren⁹⁴, M. Vessella¹⁰², M.C. Vetterli^{141,ai}, A. Vgenopoulos¹⁵¹, N. Viaux Maira^{136f}, T. Vickey¹³⁸, O.E. Vickey Boeriu¹³⁸, G.H.A. Viehhauser¹²⁵, L. Vigani^{63b}, M. Villa^{23b,23a}, M. Villaplana Perez¹⁶², E.M. Villhauer⁵², E. Vilucchi⁵³, M.G. Vinciter³⁴, G.S. Virdee²⁰, A. Vishwakarma⁵², C. Vittori^{23b,23a}, I. Vivarelli¹⁴⁵

V. Vladimirov¹⁶⁶, E. Voevodina¹⁰⁹, F. Vogel¹⁰⁸, P. Vokac¹³¹, J. Von Ahnen⁴⁸, E. Von Toerne²⁴, B. Vormwald³⁶, V. Vorobel¹³², K. Vorobev³⁷, M. Vos¹⁶², J.H. Vosseveld⁹¹, M. Vozak¹¹³, L. Vozdecky⁹³, N. Vranjes¹⁵, M. Vranjes Milosavljevic¹⁵, M. Vreeswijk¹¹³, R. Vuillermet³⁶, O. Vujinovic⁹⁹, I. Vukotic³⁹, S. Wada¹⁵⁶, C. Wagner¹⁰², W. Wagner¹⁷⁰, S. Wahdan¹⁷⁰, H. Wahlberg⁸⁹, R. Wakasa¹⁵⁶, M. Wakida¹¹⁰, V.M. Walbrecht¹⁰⁹, J. Walder¹³³, R. Walker¹⁰⁸, W. Walkowiak¹⁴⁰, A.M. Wang⁶¹, A.Z. Wang¹⁶⁹, C. Wang^{62a}, C. Wang^{62c}, H. Wang^{17a}, J. Wang^{64a}, P. Wang⁴⁴, R.-J. Wang⁹⁹, R. Wang⁶¹, R. Wang⁶, S.M. Wang¹⁴⁷, S. Wang^{62b}, T. Wang^{62a}, W.T. Wang⁷⁹, W.X. Wang^{62a}, X. Wang^{14c}, X. Wang¹⁶¹, X. Wang^{62c}, Y. Wang^{62d}, Y. Wang^{14c}, Z. Wang¹⁰⁵, Z. Wang^{62d,51,62c}, Z. Wang¹⁰⁵, A. Warburton¹⁰³, R.J. Ward²⁰, N. Warrack⁵⁹, A.T. Watson²⁰, H. Watson⁵⁹, M.F. Watson²⁰, G. Watts¹³⁷, B.M. Waugh⁹⁵, A.F. Webb¹¹, C. Weber²⁹, H.A. Weber¹⁸, M.S. Weber¹⁹, S.M. Weber^{63a}, C. Wei^{62a}, Y. Wei¹²⁵, A.R. Weidberg¹²⁵, J. Weingarten⁴⁹, M. Weirich⁹⁹, C. Weiser⁵⁴, C.J. Wells⁴⁸, T. Wenaus²⁹, B. Wendland⁴⁹, T. Wengler³⁶, N.S. Wenke¹⁰⁹, N. Wermes²⁴, M. Wessels^{63a}, K. Whalen¹²², A.M. Wharton⁹⁰, A.S. White⁶¹, A. White⁸, M.J. White¹, D. Whiteson¹⁵⁹, L. Wickremasinghe¹²³, W. Wiedenmann¹⁶⁹, C. Wiel⁵⁰, M. Wielers¹³³, N. Wieseotte⁹⁹, C. Wiglesworth⁴², L.A.M. Wiik-Fuchs⁵⁴, D.J. Wilbern¹¹⁹, H.G. Wilkens³⁶, D.M. Williams⁴¹, H.H. Williams¹²⁷, S. Williams³², S. Willocq¹⁰², P.J. Windischhofer¹²⁵, F. Winklmeier¹²², B.T. Winter⁵⁴, J.K. Winter¹⁰⁰, M. Wittgen¹⁴², M. Wobisch⁹⁶, R. Wölker¹²⁵, J. Wollrath¹⁵⁹, M.W. Wolter⁸⁵, H. Wolters^{129a,129c}, V.W.S. Wong¹⁶³, A.F. Wongel⁴⁸, S.D. Worm⁴⁸, B.K. Wosiek⁸⁵, K.W. Woźniak⁸⁵, K. Wraight⁵⁹, J. Wu^{14a,14d}, M. Wu^{64a}, M. Wu¹¹², S.L. Wu¹⁶⁹, X. Wu⁵⁶, Y. Wu^{62a}, Z. Wu^{134,62a}, J. Wuerzinger¹²⁵, T.R. Wyatt¹⁰⁰, B.M. Wynne⁵², S. Xella⁴², L. Xia^{14c}, M. Xia^{14b}, J. Xiang^{64c}, X. Xiao¹⁰⁵, M. Xie^{62a}, X. Xie^{62a}, S. Xin^{14a,14d}, J. Xiong^{17a}, I. Xiotidis¹⁴⁵, D. Xu^{14a}, H. Xu^{62a}, H. Xu^{62a}, L. Xu^{62a}, R. Xu¹²⁷, T. Xu¹⁰⁵, W. Xu¹⁰⁵, Y. Xu^{14b}, Z. Xu^{62b}, Z. Xu^{14a}, B. Yabsley¹⁴⁶, S. Yacoob^{33a}, N. Yamaguchi⁸⁸, Y. Yamaguchi¹⁵³, H. Yamauchi¹⁵⁶, T. Yamazaki^{17a}, Y. Yamazaki⁸³, J. Yan^{62c}, S. Yan¹²⁵, Z. Yan²⁵, H.J. Yang^{62c,62d}, H.T. Yang^{17a}, S. Yang^{62a}, T. Yang^{64c}, X. Yang^{62a}, X. Yang^{14a}, Y. Yang⁴⁴, Z. Yang^{62a,105}, W.-M. Yao^{17a}, Y.C. Yap⁴⁸, H. Ye^{14c}, H. Ye⁵⁵, J. Ye⁴⁴, S. Ye²⁹, X. Ye^{62a}, Y. Yeh⁹⁵, I. Yeletsikh³⁸, B.K. Yeo^{17a}, M.R. Yexley⁹⁰, P. Yin⁴¹, K. Yorita¹⁶⁷, C.J.S. Young⁵⁴, C. Young¹⁴², M. Yuan¹⁰⁵, R. Yuan^{62b,k}, L. Yue⁹⁵, X. Yue^{63a}, M. Zaazoua^{35e}, B. Zabinski⁸⁵, E. Zaid⁵², T. Zakareishvili^{148b}, N. Zakharchuk³⁴, S. Zambito⁵⁶, J.A. Zamora Saa^{136d}, J. Zang¹⁵², D. Zanzi⁵⁴, O. Zaplatilek¹³¹, S.V. Zeiβner⁴⁹, C. Zeitnitz¹⁷⁰, J.C. Zeng¹⁶¹, D.T. Zenger Jr²⁶, O. Zenin³⁷, T. Ženiš^{28a}, S. Zenz⁹³, S. Zerradi^{35a}, D. Zerwas⁶⁶, B. Zhang^{14c}, D.F. Zhang¹³⁸, G. Zhang^{14b}, J. Zhang^{62b}, J. Zhang⁶, K. Zhang^{14a,14d}, L. Zhang^{14c}, P. Zhang^{14a,14d}, R. Zhang¹⁶⁹, S. Zhang¹⁰⁵, T. Zhang¹⁵², X. Zhang^{62c}, X. Zhang^{62b}, Y. Zhang^{62c,5}, Z. Zhang^{17a}, Z. Zhang⁶⁶, H. Zhao¹³⁷, P. Zhao⁵¹, T. Zhao^{62b}, Y. Zhao¹³⁵, Z. Zhao^{62a}, A. Zhemchugov³⁸, X. Zheng^{62a}, Z. Zheng¹⁴², D. Zhong¹⁶¹, B. Zhou¹⁰⁵, C. Zhou¹⁶⁹, H. Zhou⁷, N. Zhou^{62c}, Y. Zhou⁷, C.G. Zhu^{62b}, C. Zhu^{14a,14d}, H.L. Zhu^{62a}, H. Zhu^{14a}, J. Zhu¹⁰⁵, Y. Zhu^{62c}, Y. Zhu^{62a}, X. Zhuang^{14a}, K. Zhukov³⁷, V. Zhulanov³⁷, N.I. Zimine³⁸, J. Zinsser^{63b}, M. Ziolkowski¹⁴⁰, L. Živković¹⁵, A. Zoccoli^{23b,23a}, K. Zoch⁵⁶, T.G. Zorbas¹³⁸, O. Zormpa⁴⁶, W. Zou⁴¹, L. Zwalinski³⁶.

¹Department of Physics, University of Adelaide, Adelaide; Australia.

²Department of Physics, University of Alberta, Edmonton AB; Canada.

^{3(a)}Department of Physics, Ankara University, Ankara; ^(b)Division of Physics, TOBB University of Economics and Technology, Ankara; Türkiye.

- ⁴LAPP, Université Savoie Mont Blanc, CNRS/IN2P3, Annecy; France.
- ⁵APC, Université Paris Cité, CNRS/IN2P3, Paris; France.
- ⁶High Energy Physics Division, Argonne National Laboratory, Argonne IL; United States of America.
- ⁷Department of Physics, University of Arizona, Tucson AZ; United States of America.
- ⁸Department of Physics, University of Texas at Arlington, Arlington TX; United States of America.
- ⁹Physics Department, National and Kapodistrian University of Athens, Athens; Greece.
- ¹⁰Physics Department, National Technical University of Athens, Zografou; Greece.
- ¹¹Department of Physics, University of Texas at Austin, Austin TX; United States of America.
- ¹²Institute of Physics, Azerbaijan Academy of Sciences, Baku; Azerbaijan.
- ¹³Institut de Física d'Altes Energies (IFAE), Barcelona Institute of Science and Technology, Barcelona; Spain.
- ¹⁴(^a) Institute of High Energy Physics, Chinese Academy of Sciences, Beijing; (^b) Physics Department, Tsinghua University, Beijing; (^c) Department of Physics, Nanjing University, Nanjing; (^d) University of Chinese Academy of Science (UCAS), Beijing; China.
- ¹⁵Institute of Physics, University of Belgrade, Belgrade; Serbia.
- ¹⁶Department for Physics and Technology, University of Bergen, Bergen; Norway.
- ¹⁷(^a) Physics Division, Lawrence Berkeley National Laboratory, Berkeley CA; (^b) University of California, Berkeley CA; United States of America.
- ¹⁸Institut für Physik, Humboldt Universität zu Berlin, Berlin; Germany.
- ¹⁹Albert Einstein Center for Fundamental Physics and Laboratory for High Energy Physics, University of Bern, Bern; Switzerland.
- ²⁰School of Physics and Astronomy, University of Birmingham, Birmingham; United Kingdom.
- ²¹(^a) Department of Physics, Bogazici University, Istanbul; (^b) Department of Physics Engineering, Gaziantep University, Gaziantep; (^c) Department of Physics, Istanbul University, Istanbul; (^d) Istinye University, Sariyer, Istanbul; Türkiye.
- ²²(^a) Facultad de Ciencias y Centro de Investigaciones, Universidad Antonio Nariño, Bogotá; (^b) Departamento de Física, Universidad Nacional de Colombia, Bogotá; Colombia.
- ²³(^a) Dipartimento di Fisica e Astronomia A. Righi, Università di Bologna, Bologna; (^b) INFN Sezione di Bologna; Italy.
- ²⁴Physikalisches Institut, Universität Bonn, Bonn; Germany.
- ²⁵Department of Physics, Boston University, Boston MA; United States of America.
- ²⁶Department of Physics, Brandeis University, Waltham MA; United States of America.
- ²⁷(^a) Transilvania University of Brasov, Brasov; (^b) Horia Hulubei National Institute of Physics and Nuclear Engineering, Bucharest; (^c) Department of Physics, Alexandru Ioan Cuza University of Iasi, Iasi; (^d) National Institute for Research and Development of Isotopic and Molecular Technologies, Physics Department, Cluj-Napoca; (^e) University Politehnica Bucharest, Bucharest; (^f) West University in Timisoara, Timisoara; (^g) Faculty of Physics, University of Bucharest, Bucharest; Romania.
- ²⁸(^a) Faculty of Mathematics, Physics and Informatics, Comenius University, Bratislava; (^b) Department of Subnuclear Physics, Institute of Experimental Physics of the Slovak Academy of Sciences, Kosice; Slovak Republic.

- ²⁹Physics Department, Brookhaven National Laboratory, Upton NY; United States of America.
- ³⁰Universidad de Buenos Aires, Facultad de Ciencias Exactas y Naturales, Departamento de Física, y CONICET, Instituto de Física de Buenos Aires (IFIBA), Buenos Aires; Argentina.
- ³¹California State University, CA; United States of America.
- ³²Cavendish Laboratory, University of Cambridge, Cambridge; United Kingdom.
- ³³(^a) Department of Physics, University of Cape Town, Cape Town; (^b) iThemba Labs, Western Cape; (^c) Department of Mechanical Engineering Science, University of Johannesburg, Johannesburg; (^d) National Institute of Physics, University of the Philippines Diliman (Philippines); (^e) University of South Africa, Department of Physics, Pretoria; (^f) University of Zululand, KwaDlangezwa; (^g) School of Physics, University of the Witwatersrand, Johannesburg; South Africa.
- ³⁴Department of Physics, Carleton University, Ottawa ON; Canada.
- ³⁵(^a) Faculté des Sciences Ain Chock, Réseau Universitaire de Physique des Hautes Energies - Université Hassan II, Casablanca; (^b) Faculté des Sciences, Université Ibn-Tofail, Kénitra; (^c) Faculté des Sciences Semlalia, Université Cadi Ayyad, LPHEA-Marrakech; (^d) LPMR, Faculté des Sciences, Université Mohamed Premier, Oujda; (^e) Faculté des sciences, Université Mohammed V, Rabat; (^f) Institute of Applied Physics, Mohammed VI Polytechnic University, Ben Guerir; Morocco.
- ³⁶CERN, Geneva; Switzerland.
- ³⁷Affiliated with an institute covered by a cooperation agreement with CERN.
- ³⁸Affiliated with an international laboratory covered by a cooperation agreement with CERN.
- ³⁹Enrico Fermi Institute, University of Chicago, Chicago IL; United States of America.
- ⁴⁰LPC, Université Clermont Auvergne, CNRS/IN2P3, Clermont-Ferrand; France.
- ⁴¹Nevis Laboratory, Columbia University, Irvington NY; United States of America.
- ⁴²Niels Bohr Institute, University of Copenhagen, Copenhagen; Denmark.
- ⁴³(^a) Dipartimento di Fisica, Università della Calabria, Rende; (^b) INFN Gruppo Collegato di Cosenza, Laboratori Nazionali di Frascati; Italy.
- ⁴⁴Physics Department, Southern Methodist University, Dallas TX; United States of America.
- ⁴⁵Physics Department, University of Texas at Dallas, Richardson TX; United States of America.
- ⁴⁶National Centre for Scientific Research "Demokritos", Agia Paraskevi; Greece.
- ⁴⁷(^a) Department of Physics, Stockholm University; (^b) Oskar Klein Centre, Stockholm; Sweden.
- ⁴⁸Deutsches Elektronen-Synchrotron DESY, Hamburg and Zeuthen; Germany.
- ⁴⁹Fakultät Physik, Technische Universität Dortmund, Dortmund; Germany.
- ⁵⁰Institut für Kern- und Teilchenphysik, Technische Universität Dresden, Dresden; Germany.
- ⁵¹Department of Physics, Duke University, Durham NC; United States of America.
- ⁵²SUPA - School of Physics and Astronomy, University of Edinburgh, Edinburgh; United Kingdom.
- ⁵³INFN e Laboratori Nazionali di Frascati, Frascati; Italy.
- ⁵⁴Physikalisches Institut, Albert-Ludwigs-Universität Freiburg, Freiburg; Germany.
- ⁵⁵II. Physikalisches Institut, Georg-August-Universität Göttingen, Göttingen; Germany.
- ⁵⁶Département de Physique Nucléaire et Corpusculaire, Université de Genève, Genève; Switzerland.
- ⁵⁷(^a) Dipartimento di Fisica, Università di Genova, Genova; (^b) INFN Sezione di Genova; Italy.

- ⁵⁸II. Physikalisches Institut, Justus-Liebig-Universität Giessen, Giessen; Germany.
- ⁵⁹SUPA - School of Physics and Astronomy, University of Glasgow, Glasgow; United Kingdom.
- ⁶⁰LPSC, Université Grenoble Alpes, CNRS/IN2P3, Grenoble INP, Grenoble; France.
- ⁶¹Laboratory for Particle Physics and Cosmology, Harvard University, Cambridge MA; United States of America.
- ⁶²(^a) Department of Modern Physics and State Key Laboratory of Particle Detection and Electronics, University of Science and Technology of China, Hefei; (^b) Institute of Frontier and Interdisciplinary Science and Key Laboratory of Particle Physics and Particle Irradiation (MOE), Shandong University, Qingdao; (^c) School of Physics and Astronomy, Shanghai Jiao Tong University, Key Laboratory for Particle Astrophysics and Cosmology (MOE), SKLPPC, Shanghai; (^d) Tsung-Dao Lee Institute, Shanghai; China.
- ⁶³(^a) Kirchhoff-Institut für Physik, Ruprecht-Karls-Universität Heidelberg, Heidelberg; (^b) Physikalisches Institut, Ruprecht-Karls-Universität Heidelberg, Heidelberg; Germany.
- ⁶⁴(^a) Department of Physics, Chinese University of Hong Kong, Shatin, N.T., Hong Kong; (^b) Department of Physics, University of Hong Kong, Hong Kong; (^c) Department of Physics and Institute for Advanced Study, Hong Kong University of Science and Technology, Clear Water Bay, Kowloon, Hong Kong; China.
- ⁶⁵Department of Physics, National Tsing Hua University, Hsinchu; Taiwan.
- ⁶⁶IJCLab, Université Paris-Saclay, CNRS/IN2P3, 91405, Orsay; France.
- ⁶⁷Department of Physics, Indiana University, Bloomington IN; United States of America.
- ⁶⁸(^a) INFN Gruppo Collegato di Udine, Sezione di Trieste, Udine; (^b) ICTP, Trieste; (^c) Dipartimento Politecnico di Ingegneria e Architettura, Università di Udine, Udine; Italy.
- ⁶⁹(^a) INFN Sezione di Lecce; (^b) Dipartimento di Matematica e Fisica, Università del Salento, Lecce; Italy.
- ⁷⁰(^a) INFN Sezione di Milano; (^b) Dipartimento di Fisica, Università di Milano, Milano; Italy.
- ⁷¹(^a) INFN Sezione di Napoli; (^b) Dipartimento di Fisica, Università di Napoli, Napoli; Italy.
- ⁷²(^a) INFN Sezione di Pavia; (^b) Dipartimento di Fisica, Università di Pavia, Pavia; Italy.
- ⁷³(^a) INFN Sezione di Pisa; (^b) Dipartimento di Fisica E. Fermi, Università di Pisa, Pisa; Italy.
- ⁷⁴(^a) INFN Sezione di Roma; (^b) Dipartimento di Fisica, Sapienza Università di Roma, Roma; Italy.
- ⁷⁵(^a) INFN Sezione di Roma Tor Vergata; (^b) Dipartimento di Fisica, Università di Roma Tor Vergata, Roma; Italy.
- ⁷⁶(^a) INFN Sezione di Roma Tre; (^b) Dipartimento di Matematica e Fisica, Università Roma Tre, Roma; Italy.
- ⁷⁷(^a) INFN-TIFPA; (^b) Università degli Studi di Trento, Trento; Italy.
- ⁷⁸Universität Innsbruck, Department of Astro and Particle Physics, Innsbruck; Austria.
- ⁷⁹University of Iowa, Iowa City IA; United States of America.
- ⁸⁰Department of Physics and Astronomy, Iowa State University, Ames IA; United States of America.
- ⁸¹(^a) Departamento de Engenharia Elétrica, Universidade Federal de Juiz de Fora (UFJF), Juiz de Fora; (^b) Universidade Federal do Rio De Janeiro COPPE/EE/IF, Rio de Janeiro; (^c) Instituto de

Física, Universidade de São Paulo, São Paulo;^(d) Rio de Janeiro State University, Rio de Janeiro; Brazil.

⁸² KEK, High Energy Accelerator Research Organization, Tsukuba; Japan.

⁸³ Graduate School of Science, Kobe University, Kobe; Japan.

⁸⁴(^a) AGH University of Science and Technology, Faculty of Physics and Applied Computer Science, Krakow; (^b) Marian Smoluchowski Institute of Physics, Jagiellonian University, Krakow; Poland.

⁸⁵ Institute of Nuclear Physics Polish Academy of Sciences, Krakow; Poland.

⁸⁶ Faculty of Science, Kyoto University, Kyoto; Japan.

⁸⁷ Kyoto University of Education, Kyoto; Japan.

⁸⁸ Research Center for Advanced Particle Physics and Department of Physics, Kyushu University, Fukuoka ; Japan.

⁸⁹ Instituto de Física La Plata, Universidad Nacional de La Plata and CONICET, La Plata; Argentina.

⁹⁰ Physics Department, Lancaster University, Lancaster; United Kingdom.

⁹¹ Oliver Lodge Laboratory, University of Liverpool, Liverpool; United Kingdom.

⁹² Department of Experimental Particle Physics, Jožef Stefan Institute and Department of Physics, University of Ljubljana, Ljubljana; Slovenia.

⁹³ School of Physics and Astronomy, Queen Mary University of London, London; United Kingdom.

⁹⁴ Department of Physics, Royal Holloway University of London, Egham; United Kingdom.

⁹⁵ Department of Physics and Astronomy, University College London, London; United Kingdom.

⁹⁶ Louisiana Tech University, Ruston LA; United States of America.

⁹⁷ Fysiska institutionen, Lunds universitet, Lund; Sweden.

⁹⁸ Departamento de Física Teórica C-15 and CIAFF, Universidad Autónoma de Madrid, Madrid; Spain.

⁹⁹ Institut für Physik, Universität Mainz, Mainz; Germany.

¹⁰⁰ School of Physics and Astronomy, University of Manchester, Manchester; United Kingdom.

¹⁰¹ CPPM, Aix-Marseille Université, CNRS/IN2P3, Marseille; France.

¹⁰² Department of Physics, University of Massachusetts, Amherst MA; United States of America.

¹⁰³ Department of Physics, McGill University, Montreal QC; Canada.

¹⁰⁴ School of Physics, University of Melbourne, Victoria; Australia.

¹⁰⁵ Department of Physics, University of Michigan, Ann Arbor MI; United States of America.

¹⁰⁶ Department of Physics and Astronomy, Michigan State University, East Lansing MI; United States of America.

¹⁰⁷ Group of Particle Physics, University of Montreal, Montreal QC; Canada.

¹⁰⁸ Fakultät für Physik, Ludwig-Maximilians-Universität München, München; Germany.

¹⁰⁹ Max-Planck-Institut für Physik (Werner-Heisenberg-Institut), München; Germany.

¹¹⁰ Graduate School of Science and Kobayashi-Maskawa Institute, Nagoya University, Nagoya; Japan.

¹¹¹ Department of Physics and Astronomy, University of New Mexico, Albuquerque NM; United States of America.

¹¹² Institute for Mathematics, Astrophysics and Particle Physics, Radboud University/Nikhef,

Nijmegen; Netherlands.

¹¹³Nikhef National Institute for Subatomic Physics and University of Amsterdam, Amsterdam; Netherlands.

¹¹⁴Department of Physics, Northern Illinois University, DeKalb IL; United States of America.

¹¹⁵(^a)New York University Abu Dhabi, Abu Dhabi;(^b)University of Sharjah, Sharjah; United Arab Emirates.

¹¹⁶Department of Physics, New York University, New York NY; United States of America.

¹¹⁷Ochanomizu University, Otsuka, Bunkyo-ku, Tokyo; Japan.

¹¹⁸Ohio State University, Columbus OH; United States of America.

¹¹⁹Homer L. Dodge Department of Physics and Astronomy, University of Oklahoma, Norman OK; United States of America.

¹²⁰Department of Physics, Oklahoma State University, Stillwater OK; United States of America.

¹²¹Palacký University, Joint Laboratory of Optics, Olomouc; Czech Republic.

¹²²Institute for Fundamental Science, University of Oregon, Eugene, OR; United States of America.

¹²³Graduate School of Science, Osaka University, Osaka; Japan.

¹²⁴Department of Physics, University of Oslo, Oslo; Norway.

¹²⁵Department of Physics, Oxford University, Oxford; United Kingdom.

¹²⁶LPNHE, Sorbonne Université, Université Paris Cité, CNRS/IN2P3, Paris; France.

¹²⁷Department of Physics, University of Pennsylvania, Philadelphia PA; United States of America.

¹²⁸Department of Physics and Astronomy, University of Pittsburgh, Pittsburgh PA; United States of America.

¹²⁹(^a)Laboratório de Instrumentação e Física Experimental de Partículas - LIP, Lisboa;(^b)Departamento de Física, Faculdade de Ciências, Universidade de Lisboa, Lisboa;(^c)Departamento de Física, Universidade de Coimbra, Coimbra;(^d)Centro de Física Nuclear da Universidade de Lisboa, Lisboa;(^e)Departamento de Física, Universidade do Minho, Braga;(^f)Departamento de Física Teórica y del Cosmos, Universidad de Granada, Granada (Spain);(^g)Departamento de Física, Instituto Superior Técnico, Universidade de Lisboa, Lisboa; Portugal.

¹³⁰Institute of Physics of the Czech Academy of Sciences, Prague; Czech Republic.

¹³¹Czech Technical University in Prague, Prague; Czech Republic.

¹³²Charles University, Faculty of Mathematics and Physics, Prague; Czech Republic.

¹³³Particle Physics Department, Rutherford Appleton Laboratory, Didcot; United Kingdom.

¹³⁴IRFU, CEA, Université Paris-Saclay, Gif-sur-Yvette; France.

¹³⁵Santa Cruz Institute for Particle Physics, University of California Santa Cruz, Santa Cruz CA; United States of America.

¹³⁶(^a)Departamento de Física, Pontificia Universidad Católica de Chile, Santiago;(^b)Millennium Institute for Subatomic physics at high energy frontier (SAPHIR), Santiago;(^c)Instituto de Investigación Multidisciplinario en Ciencia y Tecnología, y Departamento de Física, Universidad de La Serena;(^d)Universidad Andres Bello, Department of Physics, Santiago;(^e)Instituto de Alta Investigación, Universidad de Tarapacá, Arica;(^f)Departamento de Física, Universidad Técnica Federico Santa María, Valparaíso; Chile.

¹³⁷Department of Physics, University of Washington, Seattle WA; United States of America.

- ¹³⁸Department of Physics and Astronomy, University of Sheffield, Sheffield; United Kingdom.
- ¹³⁹Department of Physics, Shinshu University, Nagano; Japan.
- ¹⁴⁰Department Physik, Universität Siegen, Siegen; Germany.
- ¹⁴¹Department of Physics, Simon Fraser University, Burnaby BC; Canada.
- ¹⁴²SLAC National Accelerator Laboratory, Stanford CA; United States of America.
- ¹⁴³Department of Physics, Royal Institute of Technology, Stockholm; Sweden.
- ¹⁴⁴Departments of Physics and Astronomy, Stony Brook University, Stony Brook NY; United States of America.
- ¹⁴⁵Department of Physics and Astronomy, University of Sussex, Brighton; United Kingdom.
- ¹⁴⁶School of Physics, University of Sydney, Sydney; Australia.
- ¹⁴⁷Institute of Physics, Academia Sinica, Taipei; Taiwan.
- ¹⁴⁸(^a) E. Andronikashvili Institute of Physics, Iv. Javakhishvili Tbilisi State University, Tbilisi; (^b) High Energy Physics Institute, Tbilisi State University, Tbilisi; (^c) University of Georgia, Tbilisi; Georgia.
- ¹⁴⁹Department of Physics, Technion, Israel Institute of Technology, Haifa; Israel.
- ¹⁵⁰Raymond and Beverly Sackler School of Physics and Astronomy, Tel Aviv University, Tel Aviv; Israel.
- ¹⁵¹Department of Physics, Aristotle University of Thessaloniki, Thessaloniki; Greece.
- ¹⁵²International Center for Elementary Particle Physics and Department of Physics, University of Tokyo, Tokyo; Japan.
- ¹⁵³Department of Physics, Tokyo Institute of Technology, Tokyo; Japan.
- ¹⁵⁴Department of Physics, University of Toronto, Toronto ON; Canada.
- ¹⁵⁵(^a) TRIUMF, Vancouver BC; (^b) Department of Physics and Astronomy, York University, Toronto ON; Canada.
- ¹⁵⁶Division of Physics and Tomonaga Center for the History of the Universe, Faculty of Pure and Applied Sciences, University of Tsukuba, Tsukuba; Japan.
- ¹⁵⁷Department of Physics and Astronomy, Tufts University, Medford MA; United States of America.
- ¹⁵⁸United Arab Emirates University, Al Ain; United Arab Emirates.
- ¹⁵⁹Department of Physics and Astronomy, University of California Irvine, Irvine CA; United States of America.
- ¹⁶⁰Department of Physics and Astronomy, University of Uppsala, Uppsala; Sweden.
- ¹⁶¹Department of Physics, University of Illinois, Urbana IL; United States of America.
- ¹⁶²Instituto de Física Corpuscular (IFIC), Centro Mixto Universidad de Valencia - CSIC, Valencia; Spain.
- ¹⁶³Department of Physics, University of British Columbia, Vancouver BC; Canada.
- ¹⁶⁴Department of Physics and Astronomy, University of Victoria, Victoria BC; Canada.
- ¹⁶⁵Fakultät für Physik und Astronomie, Julius-Maximilians-Universität Würzburg, Würzburg; Germany.
- ¹⁶⁶Department of Physics, University of Warwick, Coventry; United Kingdom.
- ¹⁶⁷Waseda University, Tokyo; Japan.
- ¹⁶⁸Department of Particle Physics and Astrophysics, Weizmann Institute of Science, Rehovot; Israel.

- ¹⁶⁹Department of Physics, University of Wisconsin, Madison WI; United States of America.
- ¹⁷⁰Fakultät für Mathematik und Naturwissenschaften, Fachgruppe Physik, Bergische Universität Wuppertal, Wuppertal; Germany.
- ¹⁷¹Department of Physics, Yale University, New Haven CT; United States of America.
- ^a Also Affiliated with an institute covered by a cooperation agreement with CERN.
- ^b Also at An-Najah National University, Nablus; Palestine.
- ^c Also at Borough of Manhattan Community College, City University of New York, New York NY; United States of America.
- ^d Also at Bruno Kessler Foundation, Trento; Italy.
- ^e Also at Center for High Energy Physics, Peking University; China.
- ^f Also at Centro Studi e Ricerche Enrico Fermi; Italy.
- ^g Also at CERN, Geneva; Switzerland.
- ^h Also at Département de Physique Nucléaire et Corpusculaire, Université de Genève, Genève; Switzerland.
- ⁱ Also at Departament de Física de la Universitat Autònoma de Barcelona, Barcelona; Spain.
- ^j Also at Department of Financial and Management Engineering, University of the Aegean, Chios; Greece.
- ^k Also at Department of Physics and Astronomy, Michigan State University, East Lansing MI; United States of America.
- ^l Also at Department of Physics and Astronomy, University of Louisville, Louisville, KY; United States of America.
- ^m Also at Department of Physics, Ben Gurion University of the Negev, Beer Sheva; Israel.
- ⁿ Also at Department of Physics, California State University, East Bay; United States of America.
- ^o Also at Department of Physics, California State University, Sacramento; United States of America.
- ^p Also at Department of Physics, King's College London, London; United Kingdom.
- ^q Also at Department of Physics, Stanford University, Stanford CA; United States of America.
- ^r Also at Department of Physics, University of Fribourg, Fribourg; Switzerland.
- ^s Also at Department of Physics, University of Thessaly; Greece.
- ^t Also at Department of Physics, Westmont College, Santa Barbara; United States of America.
- ^u Also at Hellenic Open University, Patras; Greece.
- ^v Also at Institutio Catalana de Recerca i Estudis Avancats, ICREA, Barcelona; Spain.
- ^w Also at Institut für Experimentalphysik, Universität Hamburg, Hamburg; Germany.
- ^x Also at Institute for Nuclear Research and Nuclear Energy (INRNE) of the Bulgarian Academy of Sciences, Sofia; Bulgaria.
- ^y Also at Institute of Particle Physics (IPP); Canada.
- ^z Also at Institute of Physics and Technology, Ulaanbaatar; Mongolia.
- ^{aa} Also at Institute of Physics, Azerbaijan Academy of Sciences, Baku; Azerbaijan.
- ^{ab} Also at Institute of Theoretical Physics, Ilia State University, Tbilisi; Georgia.
- ^{ac} Also at L2IT, Université de Toulouse, CNRS/IN2P3, UPS, Toulouse; France.
- ^{ad} Also at Lawrence Livermore National Laboratory, Livermore; United States of America.
- ^{ae} Also at National Institute of Physics, University of the Philippines Diliman (Philippines); Philippines.

- af* Also at RWTH Aachen University, III. Physikalisches Institut A, Aachen; Germany.
- ag* Also at Technical University of Munich, Munich; Germany.
- ah* Also at The Collaborative Innovation Center of Quantum Matter (CICQM), Beijing; China.
- ai* Also at TRIUMF, Vancouver BC; Canada.
- aj* Also at Università di Napoli Parthenope, Napoli; Italy.
- ak* Also at University of Chinese Academy of Sciences (UCAS), Beijing; China.
- al* Also at University of Colorado Boulder, Department of Physics, Colorado; United States of America.
- am* Also at Washington College, Maryland; United States of America.
- an* Also at Yeditepe University, Physics Department, Istanbul; Türkiye.
- * Deceased